

AD-A022 349



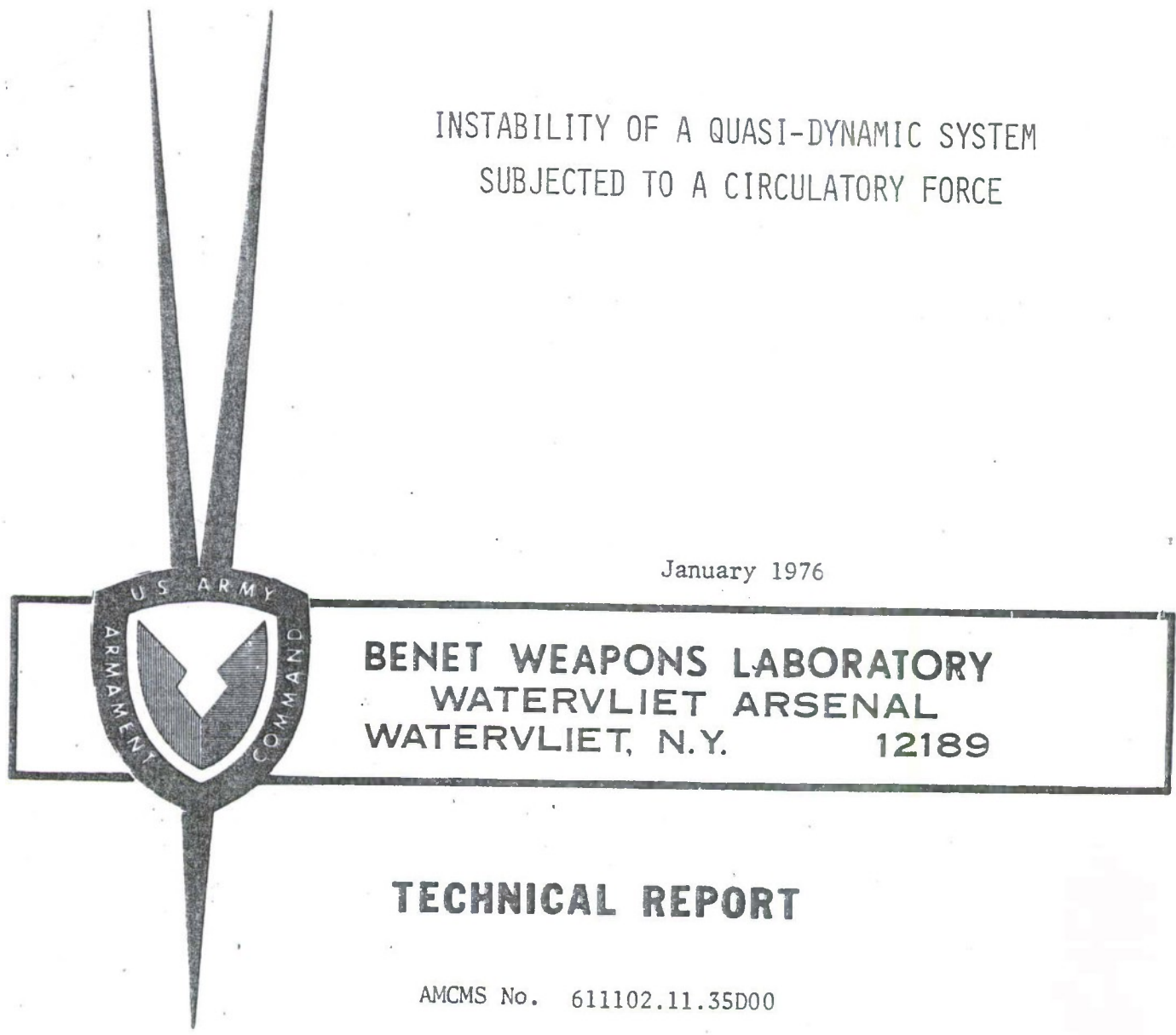
TECHNICAL LIBRARY

WVT-TR-76004

AD-A022 349

INSTABILITY OF A QUASI-DYNAMIC SYSTEM  
SUBJECTED TO A CIRCULATORY FORCE

January 1976



BENET WEAPONS LABORATORY  
WATERVLIET ARSENAL  
WATERVLIET, N.Y. 12189

TECHNICAL REPORT

AMCMS No. 611102.11.35D00

Prin No. EJ-5-Y0015-02-EJ-M7

BEST AVAILABLE COPY

APPROVED FOR PUBLIC RELEASE; DISTRIBUTION UNLIMITED

U.S. GOVERNMENT PRINTING OFFICE: 1975

DISPOSITION

Destroy this report when it is no longer needed. Do not return it to the originator.

DISCLAIMER

The findings in this report are not to be construed as an official Department of the Army position unless so designated by other authorized documents.

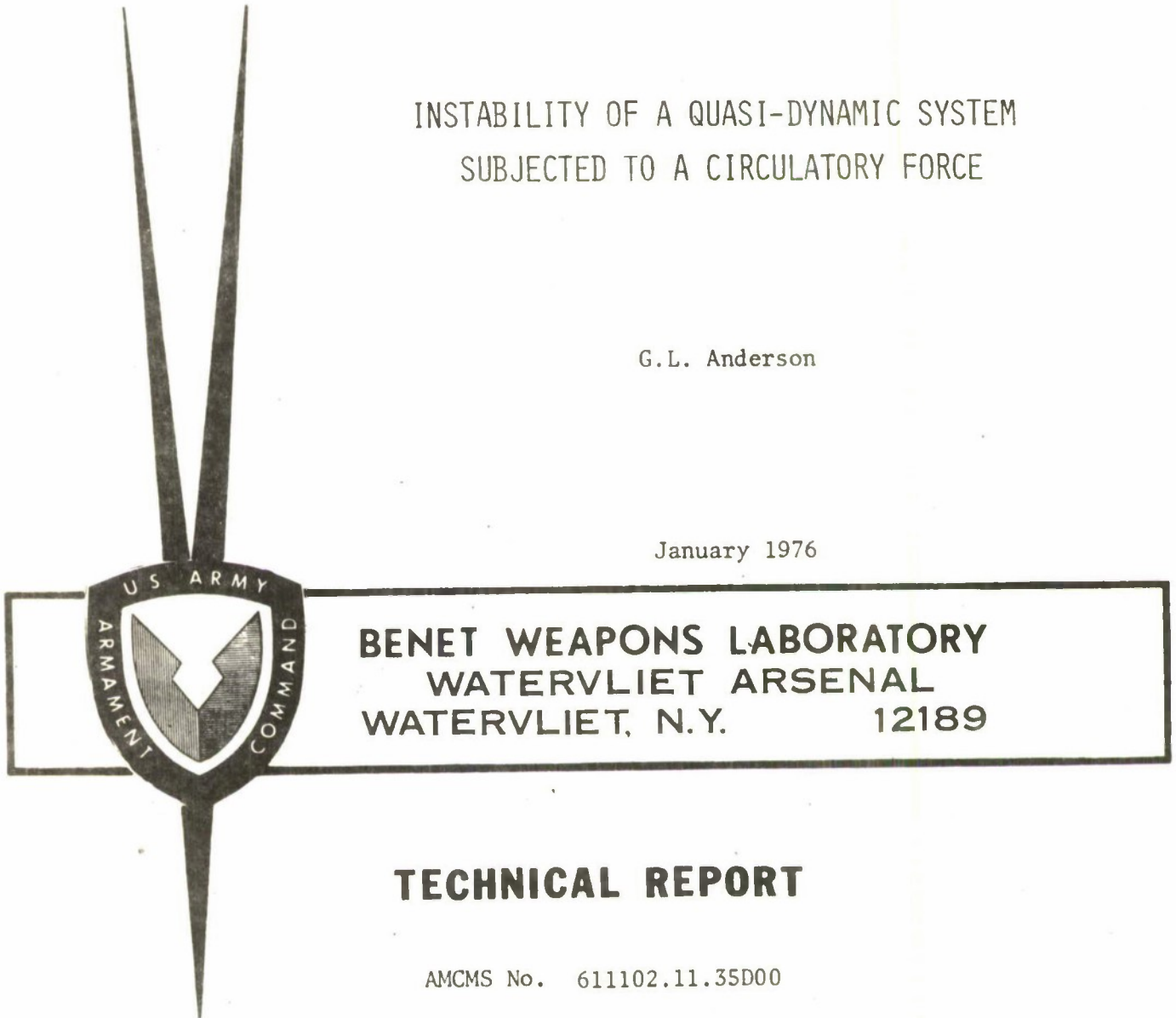
WVT-TR-76004

AD

INSTABILITY OF A QUASI-DYNAMIC SYSTEM  
SUBJECTED TO A CIRCULATORY FORCE

G.L. Anderson

January 1976



**BENET WEAPONS LABORATORY**  
**WATERVLiet ARSENAL**  
**WATERVLiet, N.Y. 12189**

**TECHNICAL REPORT**

AMCMS No. 611102.11.35D00

Pron No. EJ-5-Y0015-02-EJ-M7

APPROVED FOR PUBLIC RELEASE: DISTRIBUTION UNLIMITED

REPORT DOCUMENTATION PAGE		READ INSTRUCTIONS BEFORE COMPLETING FORM
1. REPORT NUMBER b WVT-TR-76004	2. GOVT ACCESSION NO.	3. RECIPIENT'S CATALOG NUMBER
4. TITLE (and Subtitle) INSTABILITY OF A QUASI-DYNAMIC SYSTEM SUBJECTED TO A CIRCULATORY FORCE		5. TYPE OF REPORT & PERIOD COVERED
		6. PERFORMING ORG. REPORT NUMBER
7. AUTHOR(s) G. L. Anderson		8. CONTRACT OR GRANT NUMBER(s)
9. PERFORMING ORGANIZATION NAME AND ADDRESS Benet Weapons Laboratory Watervliet Arsenal, Watervliet, N.Y. 12189 SARW-RDT		10. PROGRAM ELEMENT, PROJECT, TASK AREA & WORK UNIT NUMBERS AMCMS No. 611102.11.35D00 DA Proj. No. Pron No. EJ-5-Y0015-02-EJ-M7
11. CONTROLLING OFFICE NAME AND ADDRESS U.S. Army Armament Command Rock Island, Illinois 61201		12. REPORT DATE January 1976
		13. NUMBER OF PAGES 51
14. MONITORING AGENCY NAME & ADDRESS (if different from Controlling Office)		15. SECURITY CLASS. (of this report)  UNCLASSIFIED
		15a. DECLASSIFICATION/DOWNGRADING SCHEDULE
16. DISTRIBUTION STATEMENT (of this Report)  Approved for public release; distribution unlimited.		
17. DISTRIBUTION STATEMENT (of the abstract entered in Block 20, if different from Report)		
18. SUPPLEMENTARY NOTES		
19. KEY WORDS (Continue on reverse side if necessary and identify by block number) Damping Dynamics Flutter Stability		
20. ABSTRACT (Continue on reverse side if necessary and identify by block number) The state of stability of a double pendulum consisting of two viscoelastically hinged weightless, rigid bars carrying only a single concentrated mass and subjected to a circulatory and some conservative forces is examined. In the absence of damping in its hinges, this system, which is an example of a quasi-dynamic system, possesses multiple regions of stability and instability and can become unstable through divergence only. It is shown that the state of divergence may be attained whenever the natural frequency of the system either vanishes (see other side)		

Block 20. (cont)

or becomes infinite. When damping is present in its hinges, the system becomes unstable through either divergence characterized by a vanishing frequency or by flutter. For very slight damping, the value of the critical flutter load is less than that of the critical load of divergence whose onset is characterized by an infinite frequency in the associated non-dissipative system.

## TABLE OF CONTENTS

	Page
DD Form 1473	
Notation	iii
Introduction	1
Equations of Motion	3
The Non-Dissipative System	5
Special Cases of the Non-Dissipative System	8
The Dissipative System	12
Special Cases of the Dissipative System	15
Some Comparisons	18
Conclusions	20
References	21

## FIGURES

1. A double pendulum	22
2. Eigencurves for various values of $\alpha$	23
3. Stability map for a quasi-dynamic system ( $k_1=k_2=G=0$ )	27
4. The influence of weight on the stability of a quasi-dynamic system ( $k_1=k_2=0$ )	28
5. Stability map for the system with an end constraint ( $G=k_1=0$ )	31
6. Stability map for the system with a central constraint ( $G=k_2=0$ )	35
7. Stability map for a slightly damped system ( $k_1=k_2=G=0$ )	40
8. The influence of weight on the stability of a slightly damped system ( $k_1=k_2=0$ )	41

9. Stability map for the slightly damped system with an end constraint ( $G=k_1=0$ ) 43
10. Stability map for the slightly damped system with a central constraint ( $G=k_2=0$ ) 46

## NOTATION

$A$	inertia matrix
$A_{mn}$	elements of the inertia matrix
$b$	damping coefficient for the hinges
$C_{mn}$	elements of the stiffness matrix
$c$	spring stiffness in hinges
$D_1$	denominator in reduced frequency expression
DR	divergence region
FB	flutter boundary
$G$	$m'g\ell/c$
$g$	acceleration of gravity
$k_1, k_2$	stiffness of horizontal springs
$\ell$	length of a bar in the double pendulum
$m_1, m_2$	concentrated masses
$m'$	a mass parameter
$m, n, N$	positive integer
$N_1$	numerator in reduced frequency expression
$P$	magnitude of the applied circulatory force
$P_j$	coefficients in equation (29), $j=1,2,3,4$
$Q$	$P\ell/c$
$Q_d, Q_d^*$	critical flutter loads in the presence of arbitrary and very slight damping, respectively
$Q_{e_1}, Q_{e_2}$	critical loads of divergence of the first and second types, respectively
$\Delta Q$	difference of critical loads
$q_n$	generalized coordinates
SR	stable region
$t$	time

$\chi_n$	constants of integration
$\alpha$	tangency coefficient
$\Delta_j$	characteristic determinants, $j=1,2,3$
$\eta$	$b/\sigma c$ , dimensionless damping parameter
$\kappa_i$	$k_i \ell^2/c$ , $i=1,2$
$\lambda$	characteristic exponent
$\lambda_R, \lambda_I$	real and imaginary parts, respectively, of $\lambda$
$\mu_2$	a dimensionless mass parameter
$\sigma$	$(m' \ell^2/c)^{1/2}$
$\tau$	dimensionless time
$\phi_1, \phi_2$	angles specifying the configuration of the double pendulum
$\omega_1$	$(N_1/D_1)^{1/2}$ .

## INTRODUCTION

The differential equations of motion of a non-dissipative, non-gyroscopic system whose configuration is specified by  $N$  generalized coordinates  $q_1, q_2, \dots, q_N$  are generally of the form

$$\sum_{n=1}^N (A_{mn} \ddot{q}_n + C_{mn} \dot{q}_n) = 0, \quad m, n=1, 2, \dots, N, \quad (1)$$

where  $\ddot{q}_n = d^2 q_n / dt^2$  and  $A_{mn}$  and  $C_{mn}$  denote respectively the elements of the inertia and stiffness matrices for the system. Upon performance of equivalent operations such as multiplying the individual equations of motion by constants and adding the resulting equations to one another, the form of the set of equations in (1) can be modified. Ku<sup>1</sup> calls the system in (1) a purely dynamic system if the number of second order differential equations in (1) remains unchanged under the application of any sequence of equivalent operations. If, however, apposite equivalent operations degenerate one or more of the second order differential equations into purely algebraic equations, Ku calls such a system a quasi-dynamic system. Indeed, if the matrix  $\underset{\sim}{A} = (A_{mn})$  is non-singular, the system is purely dynamic, whereas if  $\det(\underset{\sim}{A}) = 0$ , then the system is quasi-dynamic.

In subsequent investigations, Ku<sup>2,3,4</sup> determined that a quasi-dynamic system consisting of a double pendulum composed of two elastically hinged weightless, rigid bars carrying only a single concentrated mass and subjected to a tangential force applied at its free end could lose stability only by divergence.\* Furthermore,

---

\*In the present investigation the term "divergence" means that characteristic displacements of the system grow monotonically and exponentially with time.

he showed that the onset of divergence for this particular quasi-dynamic system is characterized by its sole natural frequency of vibration becoming infinite. But, as will be demonstrated herein, these observations shed light on only one aspect of the possible stability behavior that quasi-dynamic systems are capable of exhibiting. In the present study, Ku's applied tangential force is replaced by a force whose orientation is specified by a certain tangency coefficient. It will be demonstrated here that such a system can become unstable only through divergence with the onset of instability being signaled either by the vanishing of the frequency or by the frequency becoming infinite. In addition, it will be shown that stability maps for a quasi-dynamic system often possess multiple regions of stability and divergence.

It is also of interest to investigate the influence of damping on the stability of discrete systems that have singular inertia matrices. For lack of more suitable terminology, the term "quasi-dynamic", which was applied originally only to non-dissipative systems, will be retained throughout the present discussion, where it will be understood that any non-gyroscopic system for which  $\det(\underline{A})=0$  may be called quasi-dynamic independent of the presence or absence of damping that is linearly proportional to velocity. The results reported here for the non-conservatively loaded double pendulum having a singular inertia matrix and viscoelastically hinged joints indicate, as one should expect, that internal damping has no effect whatsoever on the value of the critical load of divergence, whose onset is characterized by a vanishing frequency. In marked contrast, however, it will be shown that, for certain values of the tangency coefficient, the damped system loses

stability by flutter, whereas its non-dissipative counterpart becomes unstable by a form of divergence whose onset is characterized by a frequency becoming infinite. Furthermore, for arbitrarily small, positive internal damping, the value of the critical flutter load is observed to be less than the value of the critical divergence load for the corresponding undamped quasi-dynamic system.

### EQUATIONS OF MOTION

The double pendulum depicted in Figure 1 consists of two rigid, weightless bars of length  $\lambda$ . A concentrated mass  $m_2$  is attached to the upper bar at the point B, and the weight  $m_2g$  of this mass, where  $g$  denotes the acceleration of gravity, acts vertically downward. Frequently, in studies of the stability of a double pendulum subjected to a non-conservative force, a second mass  $m_1$  is affixed to the lower bar, often at the point B. In this study, however, it will be assumed that  $m_1=0$ , which implies immediately that the inertia matrix of the system will be singular. Thus, the system will herein be called quasi-dynamic. At the joints  $O$  and A, the double pendulum has viscoelastic hinges that exert linear restoring moments  $c\phi_1 + b\dot{\phi}_1$  and  $c(\phi_2 - \phi_1) + b(\dot{\phi}_2 - \dot{\phi}_1)$ , where  $c, b > 0$  are a stiffness coefficient and an internal damping coefficient, respectively. The system's configuration is specified by the (assumed small) angles  $\phi_1$  and  $\phi_2$  formed between the vertical and each of the bars. The points A and B are supported by horizontal linear springs of stiffness  $k_1$  and  $k_2$ , while a

compressive force  $P$  oriented at an angle  $\alpha\phi_2$  relative to the vertical, where  $\alpha$  denotes the tangency coefficient, is applied at the end B.

The equations of motion for this system may be shown to be

$$m_2 \ell^2 \ddot{\phi}_1 + 2b \dot{\phi}_1 + (2c - P\ell + k_1 \ell^2 + k_2 \ell^2 - m_2 g \ell) \phi_1 + m_2 \ell^2 \ddot{\phi}_2 - b \dot{\phi}_2 - (c - k_2 \ell^2 - \alpha P \ell) \phi_2 = 0, \quad (2)$$

$$m_2 \ell^2 \ddot{\phi}_1 - b \dot{\phi}_1 - (c - k_2 \ell^2) \phi_1 + m_2 \ell^2 \ddot{\phi}_2 + b \dot{\phi}_2 + [c - P\ell(1 - \alpha) + k_2 \ell^2 - m_2 g \ell] \phi_2 = 0, \quad (3)$$

where  $\dot{\phi}_1 = d\phi_1/dt$ , etc. To facilitate the analysis of these equations, it is expedient to render them in dimensionless form. Defining  $m_2 = \mu_2 m'$ ,  $Q = P\ell/c$ ,  $\kappa_j = k_j \ell^2/c$ ,  $G = m' g \ell/c$ ,  $\eta = b/\sigma c$ , and  $t = \sigma \tau$ , where  $j=1,2$  and  $\sigma^2 = m' \ell^2/c$ , one finds that (2) and (3) become

$$\mu_2 \ddot{\phi}_1 + 2\eta \dot{\phi}_1 + (2 - Q + \kappa_1 + \kappa_2 - \mu_2 G) \phi_1 + \mu_2 \ddot{\phi}_2 - \eta \dot{\phi}_2 - (1 - \alpha Q - \kappa_2) \phi_2 = 0, \quad (4)$$

$$\mu_2 \ddot{\phi}_1 - \eta \dot{\phi}_1 - (1 - \kappa_2) \phi_1 + \mu_2 \ddot{\phi}_2 + \eta \dot{\phi}_2 + [1 + Q(\alpha - 1) + \kappa_2 - \mu_2 G] \phi_2 = 0, \quad (5)$$

where now  $\phi_1 = d\phi_1/d\tau$  etc. The elements of the inertia matrix  $\underline{A}$  associated with (4) and (5) are, clearly,  $A_{mn} = \mu_2$  for  $m, n=1,2$ . Hence,  $\underline{A}$  is singular.

## THE NON-DISSIPATIVE SYSTEM

If no damping is present in the hinges, then  $\eta_1 = \eta_2 = 0$  and (4) and (5) reduce to

$$\mu_2 \ddot{\phi}_1 + (2 - Q + \kappa_1 + \kappa_2 - \mu_2 G) \phi_1 + \mu_2 \ddot{\phi}_2 - (1 - \alpha Q - \kappa_2) \phi_2 = 0, \quad (6)$$

$$\mu_2 \ddot{\phi}_1 - (1 - \kappa_2) \phi_1 + \mu_2 \ddot{\phi}_2 + [1 + Q(\alpha - 1) + \kappa_2 - \mu_2 G] \phi_2 = 0. \quad (7)$$

If (7) is subtracted from (6), one finds that the inertia terms  $\mu_2 \ddot{\phi}_1$  and  $\mu_2 \ddot{\phi}_2$  cancel and that a purely algebraic relationship, namely,

$$\phi_2 = (3 + \kappa_1 - \mu_2 G - Q) \phi_1 / (2 - \mu_2 G - Q), \quad (8)$$

exists between  $\phi_1$  and  $\phi_2$ . Ku<sup>1</sup> calls a relationship of the type in (8) an internal constraint.

Inserting (8) into either of the differential equations in (6) or (7), one obtains the following reduced equation of motion for the quasi-dynamical system:

$$\ddot{\phi}_1 + \omega_1^2 \phi_1 = 0, \quad (9)$$

where

$$\omega_1^2 = N_1 / D_1 \quad (10)$$

with

$$N_1 = (1 - \alpha)Q^2 - [(1 - \alpha)(3 + \kappa_1 - \mu_2 G) - \mu_2 G + 2\kappa_2]Q + 1 + \kappa_1 + \kappa_2(5 + \kappa_1) - \mu_2 G(3 + \kappa_1 + 2\kappa_2) + (\mu_2 G)^2 \quad (11)$$

and

$$D_1 = \mu_2(5 + \kappa_1 - 2\mu_2 G - 2Q). \quad (12)$$

It is obvious from (9) that the motion of the system is characterized by a single natural frequency  $\omega_1$ . Consequently, the occurrence of flutter, which ensues upon the coalescence of two natural frequencies when the loading conditions are suitable, is impossible in the quasi-dynamic system considered here even if its purely dynamic counterpart is flutter prone for a given circulatory force. Therefore, the state of stability of the given quasi-dynamic system can now be determined from the algebraic sign of  $\omega_1^2$ .

If  $\omega_1^2 > 0$ , it is evident from (9) that the motion of the system is stable since it consists of a bounded simple harmonic oscillation. On the other hand, if  $\omega_1^2 < 0$ , the motion grows exponentially in time; hence the system is unstable through divergence. In view of (10), it can now be stated the given quasi-dynamic system will be stable whenever  $N_1$  and  $D_1$  have the same algebraic sign and unstable by divergence whenever  $N_1$  and  $D_1$  have opposite signs. The boundaries of the regions of stability and instability in stability map can be obtained from the conditions

$$N_1 = D_1 = 0. \quad (13)$$

For certain combinations of parameters, however, it happens that  $N_1$  cannot vanish. In such cases, the stability boundary is determined from only one of the conditions in (13), namely,

$$D_1 = 0. \quad (14)$$

If  $D_1$  is persistent in sign while  $N_1$  changes sign as  $Q$  is increased, the system becomes unstable by divergence and the critical divergence load may be computed from the condition of vanishing frequency, i.e.,  $\omega_1^2=0$ , which implies that  $N_1=0$ . Instability whose onset is characterized by the vanishing of  $\omega_1^2$  will be called here divergence of the first type. It may also be remarked that a rather unusual feature of the present quasi-dynamic system is that its motion can become divergent even though  $\omega_1^2$  does not vanish when the sign of  $\omega_1^2$  is changed from positive to negative as the value of the load parameter  $Q$  is increased up to and beyond its critical value. Specifically, suppose that, for a given value of  $Q$ , both  $N_1$  and  $D_1$  are positive. If, upon increasing  $Q$ ,  $N_1$  remains positive while  $D_1$  becomes negative, then  $N_1$  and  $D_1$  have opposite signs. Thus, the motion of the system must be divergent. Clearly, the value of  $\omega_1^2$  does not vanish at the onset of instability, but it does become infinite. This phenomenon is termed divergence of the second type. If both  $N_1$  and  $D_1$  vanish for some value of  $Q$ , then the value of  $\omega_1^2$  must be obtained with the aid of L'Hôpital's rule. In references [2]-[4], Ku discussed only divergence of the second type since the system that he studied was subjected to a tangential force which cannot produce divergence of the first type.

## SPECIAL CASES OF THE NON-DISSIPATIVE SYSTEM

The following special systems will be considered in some detail:  
 (a)  $G=\kappa_1=\kappa_2=0$ , the effect of weight is ignored and the two horizontal springs are absent; (b)  $\kappa_1=\kappa_2=0$ , the effect of weight is retained but the horizontal springs are absent; (c)  $G=\kappa_1=0$ , the spring at B in Figure 1 is included in the system but the effect of weight is ignored and the spring at A is absent; (d)  $G=\kappa_2=0$ , the spring at A is present in the system, whereas the effect of weight is ignored and the spring at B is absent.

For Case a, (11) and (12) become

$$N_1 = (1-\alpha)Q^2 - 3(1-\alpha)Q + 1, \quad (15)$$

$$D_1 = \mu_2(5-2Q), \quad (16)$$

so that (10) can be expressed as

$$\omega_1^2 = [(1-\alpha)Q^2 - 3(1-\alpha)Q+1]/\mu_2(5-2Q). \quad (17)$$

Let  $Q_{e_1}$  and  $Q_{e_2}$  denote the critical loads of divergence of the first and second types, respectively. Then, to determine the stability boundaries, the conditions in (13) in conjunction with (15) and (16) yield

$$(1-\alpha)Q_{e_1}^2 - 3(1-\alpha)Q_{e_1} + 1 = 0, \quad (18)$$

and

$$Q_{e_2} = 5/2. \quad (19)$$

Equation (18) was first studied by Herrmann and Bungay<sup>5</sup>, and (19) was obtained in references [2]-[4] in the special case of  $\alpha=1$ .

To identify the regions of stability and instability for the given system, one need only examine the eigencurves obtained from (17). Representative eigencurves prepared with  $\mu_2=1$  (with no loss of generality are shown in Figure 2 for four values of the tangency coefficient  $\alpha$ . These eigencurves consist of two branches which asymptotically approach the horizontal line  $Q=5/2$  as  $\omega_1^2 \rightarrow \pm\infty$ . For a given value of  $\alpha$ , these eigencurves reveal the possibility of multiple intervals of stability and instability relative to the load parameter  $Q$ . The case of  $\alpha=1/5$  is exceptional, however, because (17) assumes the rather simple form  $\omega_1^2 = \frac{1}{2}(1-2Q)$ . Hence, it is clear that  $\omega_1^2$  decreases linearly in  $Q$  and the system loses stability by divergence of the first type at  $Q=1/2$ . A stability map in the  $Q\alpha$ -plane that is obtained from (18) and (19) appears in Figure 3. The various stable regions (SR) and divergence regions (DR) have been identified with the aid of the eigencurves shown in Figure 2.

As a second example, consider the double pendulum in a gravity field ( $G \neq 0$ ), case b. In the discussion that follows, both positive and negative values of  $G$ , referring to either a vertically upright and a vertically hanging double pendulum, respectively, will be considered. Under the assumptions that  $\kappa_1 = \kappa_2 = 0$  and  $\mu_2 = 1$ , (11)-(13) yield

$$(1-\alpha)Q_{e_1}^2 - [(1-\alpha)(3-G)-G]Q_{e_1} + 1 - 3G + G^2 = 0, \quad (20)$$

$$Q_{e_2} = \frac{1}{2} (5-2G), \quad (21)$$

the latter being a straight line having a slope of -1 in the QG-plane. When  $\alpha=1$ , (20) leads to

$$Q_{e_1} = - (1-3G + G^2)/G. \quad (22)$$

In Figure 4, stability maps in the QG-plane, as obtained from (20)-(22) are presented for  $\alpha=0, 3/4$ , and 1. In Figure 4a, all the stability boundaries are parallel straight lines, namely, that given in (21) as well as  $Q = \frac{1}{2} (3 \pm \sqrt{5} - 2G)$ , which are obtained from (20) when  $\alpha=0$ . Upon examining the appropriate eigencurves for the given system, one can conclude that the stability maps shown in Figure 4 possess multiple regions of stability and divergence, whose boundaries depend strongly upon the weight parameter G and the tangency coefficient  $\alpha$ .

For a non-conservatively loaded double pendulum whose motion (case c) is constrained by the presence of a horizontal linear restoring spring acting at its upper end B, as depicted in Figure 1, the stability boundaries are derivable from

$$(1-\alpha)Q_{e_1}^2 - [3(1-\alpha) + 2\kappa_2]Q_{e_1} + 1 + 5\kappa_2 = 0, \quad (23)$$

$$Q_{e_2} = 5/2. \quad (24)$$

Equation (23) was previously given by Sundararajan<sup>6</sup>, and (24) is identical to (19) which was obtained for the system in which the end support was absent. The stability boundaries found from (23)-(24) are plotted in Figure 5 for  $\alpha=0, 1/4, 1$ , and  $3/2$ . It is evident that the forms of these curves are very significantly

influenced by the values of the elastic constraint parameter  $\kappa_2$  and the tangency coefficient  $\alpha$ .

In the case just described, the stability boundary obtained from (24) is merely a horizontal straight line which is independent of  $\kappa_2$ . By contrast, if the spring is removed from the end B (see Figure 1) and is instead attached horizontally at the hinge A in the double pendulum, (11)-(13) yield, for case d,

$$(1-\alpha)Q_{e_1}^2 - (1-\alpha)(3+\kappa_1)Q_{e_1} + 1 + \kappa_1 = 0, \quad (25)$$

and

$$Q_{e_2} = \frac{1}{2} (5+\kappa_1). \quad (26)$$

It should be noted that when  $\alpha=1$ , (10) becomes

$$\omega_1^2 = (1+\kappa_1)/\mu_2(5+\kappa_1-2Q).$$

Consequently, in the case of a tangential force, stability is lost only through divergence of the second type with the critical divergence load being obtainable from (24).

The stability boundaries obtained from (25) and (26) have been plotted in the stability maps in Figure 6 for five values of  $\alpha$ , where multiple regions of stability and divergence, whose extents depend strongly upon  $\alpha$ , are shown. The secondary (upper) stability regions appearing in Figure 6 change their character in the sense of separating from each other as the value of  $\alpha$  is increased through and beyond  $\alpha=1/2$ . Indeed, for  $\alpha=1/2$ , (25) assumes the form

$$Q_{e_1}^2 - (3+\kappa_1)Q_{e_1} + 2(1+\kappa_1) = 0,$$

whence

$$Q_{e_1} = \frac{1}{2} (3 + \kappa_1 \pm |\kappa_1 - 1|). \quad (27)$$

Selecting the negative sign in (27), one finds

$$Q_{e_1} = \begin{cases} 1 + \kappa_1 & \text{if } 0 \leq \kappa_1 \leq 1, \\ 2 & \text{if } 1 \leq \kappa_1, \end{cases}$$

whereas, upon choosing the positive sign,

$$Q_{e_1} = \begin{cases} 2 & \text{if } 0 \leq \kappa_1 \leq 1, \\ 1 + \kappa_1 & \text{if } 1 \leq \kappa_1. \end{cases}$$

Therefore, these two expressions lead, in essence, to a pair of intersecting straight lines, as shown in Figure 6c, which form the boundaries of the secondary region of stability.

#### THE DISSIPATIVE SYSTEM

A solution of the set of homogeneous equations (4) and (5), in which the damping terms have been retained, will be sought in the form

$$\phi_n(\tau) = X_n e^{\lambda \tau}, \quad n=1,2, \quad (28)$$

where the  $X_n$ 's are constants and the characteristic exponent  $\lambda$  is, in general, a complex number, i.e.,  $\lambda = \lambda_R + i\lambda_I$ , where  $i = (-1)^{1/2}$ .

Substitution of (28) into (4) and (5) leads to a set of linear homogeneous equations from which is derived in the familiar manner the frequency equation

$$p_1 \lambda^3 + p_2 \lambda^2 + p_3 \lambda + p_4 = 0, \quad (29)$$

where

$$\begin{aligned} p_1 &= 5\mu_2\eta, & p_2 &= \mu_2(5+\kappa_1-2\mu_2G-2Q) + \eta^2, \\ p_3 &= \eta[2+\kappa_1+5\kappa_2-3\mu_2G+3Q(\alpha-1)], & (30) \\ p_4 &= 1 + \kappa_1 + 5\kappa_2 + \kappa_1\kappa_2 - \mu_2G(3+\kappa_1+2\kappa_2) + (\mu_2G)^2 + \\ &+ Q[(3+\kappa_1)(\alpha-1)-2\kappa_2 + (2-\alpha)\mu_2G] + Q^2(1-\alpha). \end{aligned}$$

In view of the form of equation (28), it is clear that the motion of the system will be stable if all three values of  $\lambda$  obtained from (29) are such that  $\lambda_R < 0$ . On the other hand, if  $\lambda_R > 0$  and  $\lambda_I = 0$  for at least one of the three characteristic roots, the system will be unstable by divergence, whereas, if  $\lambda_R > 0$  and  $\lambda_I \neq 0$ , for at least one of the roots of (29), the motion consists of an oscillation with an exponentially increasing amplitude, and the equilibrium configuration of the system is said to be unstable by flutter.

The Routh-Hurwitz criterion states that the necessary and sufficient conditions for all the roots  $\lambda_j$ ,  $j=1,2,3$ , of (29) to have negative real parts is that  $p_1 > 0$  and all the determinants

$$\Delta_1 = p_2, \quad \Delta_2 = \begin{vmatrix} p_2 & p_1 \\ p_4 & p_3 \end{vmatrix}, \quad \Delta_3 = \begin{vmatrix} p_2 & p_1 & 0 \\ p_4 & p_3 & p_2 \\ 0 & 0 & 0 \end{vmatrix}$$

be positive, i.e.,

$$p_1 > 0, \quad p_2 > 0, \quad p_2 p_3 - p_1 p_4 > 0, \quad p_4 > 0, \quad (31)$$

since  $\Delta_3 = p_4 \Delta_2$ . In view of (30), the inequalities in (31) become

$$p_1 = 5\mu_2 \eta > 0,$$

$$p_2 = \mu_2(5 + \kappa_1 - 2\mu_2 G - 2Q) + \eta^2 > 0,$$

$$\begin{aligned} p_2 p_3 - p_1 p_4 &= \eta \{ \mu_2 [(2 - \mu_2 G)^2 + (1 + \kappa_1)^2] + \eta^2 [2 + \kappa_1 + 5\kappa_2 - 3\mu_2 G] - \\ &\quad - [4 + 2\kappa_1 - \mu_2 G - (1 - \alpha)(2\kappa_1 + \mu_2 G - 3\eta^2)] Q + \\ &\quad + \mu_2 (1 - \alpha) Q^2 \} > 0, \end{aligned} \quad (32)$$

$$\begin{aligned} p_4 &= 1 + \kappa_1 + 5\kappa_2 + \kappa_1 \kappa_2 - \mu_2 G(3 + \kappa_1 + 2\kappa_2) + (\mu_2 G)^2 - \\ &\quad - [(3 + \kappa_1)(1 - \alpha) + 2\kappa_2 - (2 - \alpha)\mu_2 G] Q + (1 - \alpha) Q^2 > 0. \end{aligned}$$

In the present case, the critical flutter load  $Q_d$  is determined from the condition  $p_2 p_3 - p_1 p_4 = 0$ , which, in view of (32), becomes as long as  $\eta > 0$

$$\begin{aligned} (1 - \alpha) Q_d^2 - [4 + 2\kappa_1 - G - (1 - \alpha)(2\kappa_1 + G - 3\eta^2)] Q_d + (2 - G)^2 + \\ + (1 + \kappa_1)^2 + \eta^2 [2\kappa_1 + 5\kappa_2 - 3G] = 0, \end{aligned} \quad (33)$$

upon setting  $\mu_2 = 1$ , with no loss of generality for present purposes.

In the case of a tangential force ( $\alpha=1$ ), (33) yields

$$Q_d = [(2-G)^2 + (1+\kappa_1)^2 + \eta^2(2+\kappa_1+5\kappa_2-3G)] / (4+2\kappa_1-G). \quad (34)$$

#### SPECIAL CASES OF THE DISSIPATIVE SYSTEM

In analogy with the special cases (a)-(d) of the non-dissipative system discussed in an earlier section, attention may now be turned to the corresponding situations for the dissipative system, namely,

Case a.  $G = \kappa_1 = \kappa_2 = 0$ :

$$(1-\alpha)Q_d^2 - [4+3\eta^2(1-\alpha)]Q_d + 5 + 2\eta^2 = 0; \quad (35)$$

Case b.  $\kappa_1 = \kappa_2 = 0$ :

$$(1-\alpha)Q_d^2 - [4-G-(1-\alpha)(G-3\eta^2)]Q_d + 1 + (2-G)^2 + \eta^2(2-3G) = 0; \quad (36)$$

Case c.  $\kappa_1 = G = 0$ :

$$(1-\alpha)Q_d^2 - [4+3\eta^2(1-\alpha)]Q_d + 5 + \eta^2(2+5\kappa_2) = 0; \quad (37)$$

Case d.  $\kappa_2 = G = 0$ :

$$(1-\alpha)Q_d^2 - [4+2\alpha\kappa_1 + 3\eta^2(1-\alpha)]Q_d + 4 + (1+\kappa_1)^2 + \eta^2(2+\kappa_1) = 0. \quad (38)$$

In the event that the applied load is a tangential force ( $\alpha=1$ ), (35)-(38) yield

$$Q_d = (5 + 2\eta^2)/4, \quad (39)$$

$$Q_d = [1 + (2-G)^2 + \eta^2(2-3G)]/(4-G), \quad (40)$$

$$Q_d = [5 + \eta^2(2 + 5\kappa_2)]/4, \quad (41)$$

$$Q_d = [4 + (1 + \kappa_1)^2 + \eta^2(2 + \kappa_1)]/2(2 + \kappa_1), \quad (42)$$

respectively.

In Figure 7, the stability map, i.e., a plot of the variation of the critical load  $Q$  versus the tangency coefficient  $\alpha$ , has been prepared for the case of a double pendulum for which  $G = \kappa_1 = \kappa_2 = 0$ , case a. The solid curves form the divergence boundaries (DB) associated with divergence of the first type, and these boundaries are completely independent of the value of the damping parameter  $\eta$ . The dot-dash curve, associated with instability due to divergence of the second type, also represents a divergence boundary which, however, is obtained only in the complete absence of damping ( $\eta=0$ ). If damping is present ( $\eta>0$ ) in the system, divergence of the second type no longer occurs, but now instability due to flutter appears in its place. The dash-dash curve, which provides the flutter boundary (FB), is obtained from

$$(1-\alpha)Q_d^{*2} - 4Q_d^* + 5 = 0 \quad (\alpha \neq 1) \quad (43)$$

which results from (43) in the case of slight damping, i.e.,  $0 < \eta \ll 1$ , or from  $Q_d^* = 5/4$  when  $\alpha = 1$  which is found from (39) upon neglecting  $\eta$ .

If  $\eta = 0$ , the stability region (SR) is bounded by the solid and dot-dash curves. For the slightly damped system ( $0 < \eta \ll 1$ ), the solid curves are still pertinent, but now the dot-dash curve, corresponding to divergence of the second type, is not since the dot-dash divergence boundary must be replaced by the dash-dash flutter boundary. Upon examination of (18) and Figure 7, it is evident that flutter is possible only when  $\alpha > 5/9$  and  $\eta > 0$ . If  $\alpha < 5/9$ , the system becomes unstable by divergence of the first type. Furthermore, it is obvious that  $Q_d < Q_{e_2}$ .

In Case b, (40) becomes

$$(1-\alpha)Q_d^{*2} - (4-G)Q_d^* + 1 + (2-G)^2 = 0$$

when  $0 < \eta \ll 1$ . Stability maps in the QG-plane are shown in Figure 8 for  $\alpha = 3/4$  and  $\alpha = 1$ . In both cases, the stability boundary consists of a flutter boundary and a divergence boundary which intersect at a point in the first quadrant.

If the upper end of the spring is supported by a spring ( $\kappa_2 \neq 0$ ), then, with  $\kappa_1 = G = 0$ , (41) is appropriate, and for very slight damping this equation becomes identical to (43). Therefore, in the presence of slight internal damping, the value of the critical flutter load is independent of the spring stiffness parameter  $\kappa_2$ . The flutter boundaries, consequently, are identified by the horizontal dash-dash lines in Figures 9a-c, which have been prepared for  $\alpha = 1/4, 1, \text{ and } 3/2$ , respectively.

Finally, the flutter boundary for a slightly damped double pendulum supported by a spring at the central hinge may be determined from

$$(1-\alpha)Q_d^{*2} - 2(2+\alpha\kappa_1)Q_d^* + 4 + (1+\kappa_1)^2 = 0$$

which is obtained from (42) upon neglecting the terms containing  $\eta$ . Two stability maps in the  $Q\kappa_1$ -plane are presented in Figure 10 for  $\alpha=0.504$  and  $\alpha=3/5$ .

#### SOME COMPARISONS

In the case of a tangential force,  $\alpha=1$ , (34) becomes

$$Q_d^* = [(2-G)^2 + (1+\kappa_1)^2]/(4+2\kappa_1-G) \quad (44)$$

for very slight damping, i.e.,  $0 < \eta \ll 1$ . For the corresponding undamped system, one has

$$Q_{e_2} = \frac{1}{2} (5 + \kappa_1 - 2G), \quad (45)$$

upon setting  $D_1=0$  and  $\mu_2=1$  in (12). The difference of these quantities is easily shown to be

$$\begin{aligned} \Delta Q &= Q_{e_2} - Q_d^* \\ &= 5(1+\kappa_1)(2-G)/2(4+2\kappa_1-G). \end{aligned} \quad (46)$$

If  $G=0$ , then (46) becomes  $\Delta Q=5(1+\kappa_1)/2(2+\kappa_1)$ , which is always positive for  $\kappa_1 \geq 0$ . Thus,  $Q_d^* < Q_{e_2}$ . If, on the other hand,  $\kappa_1=0$ , then (46) yields

$$\Delta Q = 5(2-G)/2(4-G), \quad (47)$$

which is meaningful only for  $G \leq 2/3$ .<sup>\*</sup> Thus, it follows from (47) that  $\Delta Q \geq 1$  for  $G \leq 2/3$ . Consequently,  $Q_d^* < Q_{e_2}$ . Therefore, one may conclude, in the case of a tangential force, that the value of the critical flutter load for the slightly damped quasi-dynamic system is always less than the value of the critical load of divergence of the second type for its undamped counterpart.

In the other extreme of very large damping, it follows from (34) for a tangential force that an approximation for the critical flutter load is

$$Q_d \sim \eta^2(2+\kappa_1+5\kappa_2-3G)/(4+2\kappa_1-G), \quad (48)$$

from which it is clear that the value of  $Q_d$  is essentially proportional to the square of the internal damping parameter  $\eta$ . In contrast, one can show that the two solutions of (33) behave as  $Q_d \sim 3\eta^2$  and

$$Q_d \sim (2+\kappa_1+5\kappa_2-3G)/3(1-\alpha) \quad (49)$$

as  $\eta \rightarrow \infty$ , provided that  $\alpha \neq 1$ . Equation (49) yields the critical flutter load for very large  $\eta$ , and, in addition, it also yields the maximum critical value of  $Q_d$  when  $Q_d$  is treated as a function of  $\eta$ .

---

<sup>\*</sup>This value of  $G$  is obtained from  $3G^2-8G+4=0$  which results when  $Q_d^*$  in (44) with  $\kappa_1=0$  is equated to  $Q_{e_1}$  in (22). Thus,  $G=2/3$  is the abscissa of the point in the  $QG$ -plane in Figure 8b at which the flutter boundary and the divergence (of the first type) boundary intersect.

It is obvious from (48) that, for a double pendulum subjected to a tangential force, sufficiently large damping raises the value of  $Q_d$  beyond that of  $Q_{e_2}$  as given in (45). However, it should be remarked that, under certain circumstances, even very large damping may be of a destabilizing nature when  $\alpha \neq 1$ . For example, suppose that  $\kappa_2 = G = 0$ , so that the difference of (49) and (45) is

$$\Delta Q = [11 + \kappa_1 - 3\alpha(5 + \kappa_1)]/6(1 - \alpha). \quad (50)$$

In the event that  $\alpha = 3/5$  (for the sake of being specific), (50) becomes  $\Delta Q = (5 - 2\kappa_1)/6$ . Hence, for sufficiently large  $n$ ,  $Q_d \leq Q_{e_2}$  whenever  $\kappa_1 \leq 5/2$  and  $Q_{e_2} < Q_d$  whenever  $\kappa_1 > 5/2$ .

## CONCLUSIONS

By means of example, it has been shown that a non-dissipative, quasi-dynamic system composed of a certain double pendulum subjected to a circulatory force and some conservative forces can lose stability only by divergence. Two modes of onset of divergence have been identified: one associated with a vanishing natural frequency and the other with a natural frequency becoming infinite. Multiple regions of stability and instability were observed in apposite stability maps. However, if frictional forces are acting in the hinges of the double pendulum, the secondary stable regions disappear and the second mode of divergence is replaced by loss of stability due to flutter. Furthermore, if the damping forces are arbitrarily small, the value of the critical flutter load  $Q_d^*$  was found to be always less than the critical divergence load  $Q_{e_2}$  for the corresponding undamped system. In addition to the results reported here, still other aspects of certain quasi-dynamic systems have been discussed in references [7]-[10].

## REFERENCES

1. A. B. KU, Zeit. angew. Math. Phys. 20, 986 (1971).
2. A. B. KU, Int. J. Mech. Sci. 15, 905 (1973).
3. A. B. KU, Developments in Mechanics 7, 449 (1973).
4. A. B. KU, Developments in Mechanics 8, 251 (1975).
5. G. HERRMANN and R. W. BUNGAY, J. appl. Mech. 31, 435 (1964).
6. C. SUNDARARAJAN, J. Appl. Mech. 41, 313 (1974).
7. C. ORAN, J. Appl Mech., 37, 671 (1970).
8. H. ZIEGLER, In Instability of Continuous Systems, edited by H. Leipholz. Springer-Verlag, New York (1971).
9. C. ORAN, J. Appl. Mech., 39, 263 (1972).
10. Y. SUGIYAMA, K. KASHIMA, and H. KAWAGOE, submitted for publication.

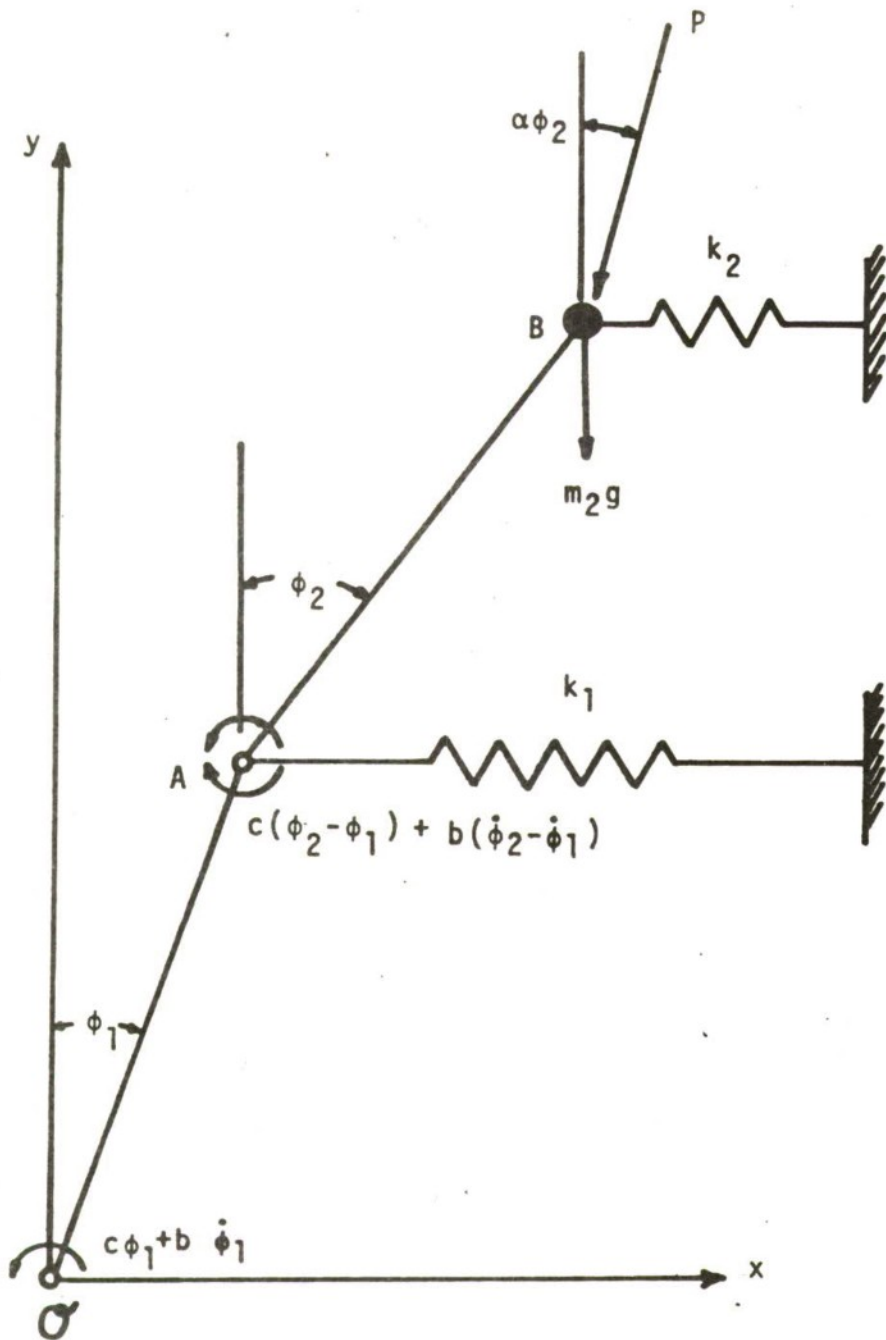


Figure 1. A double pendulum.

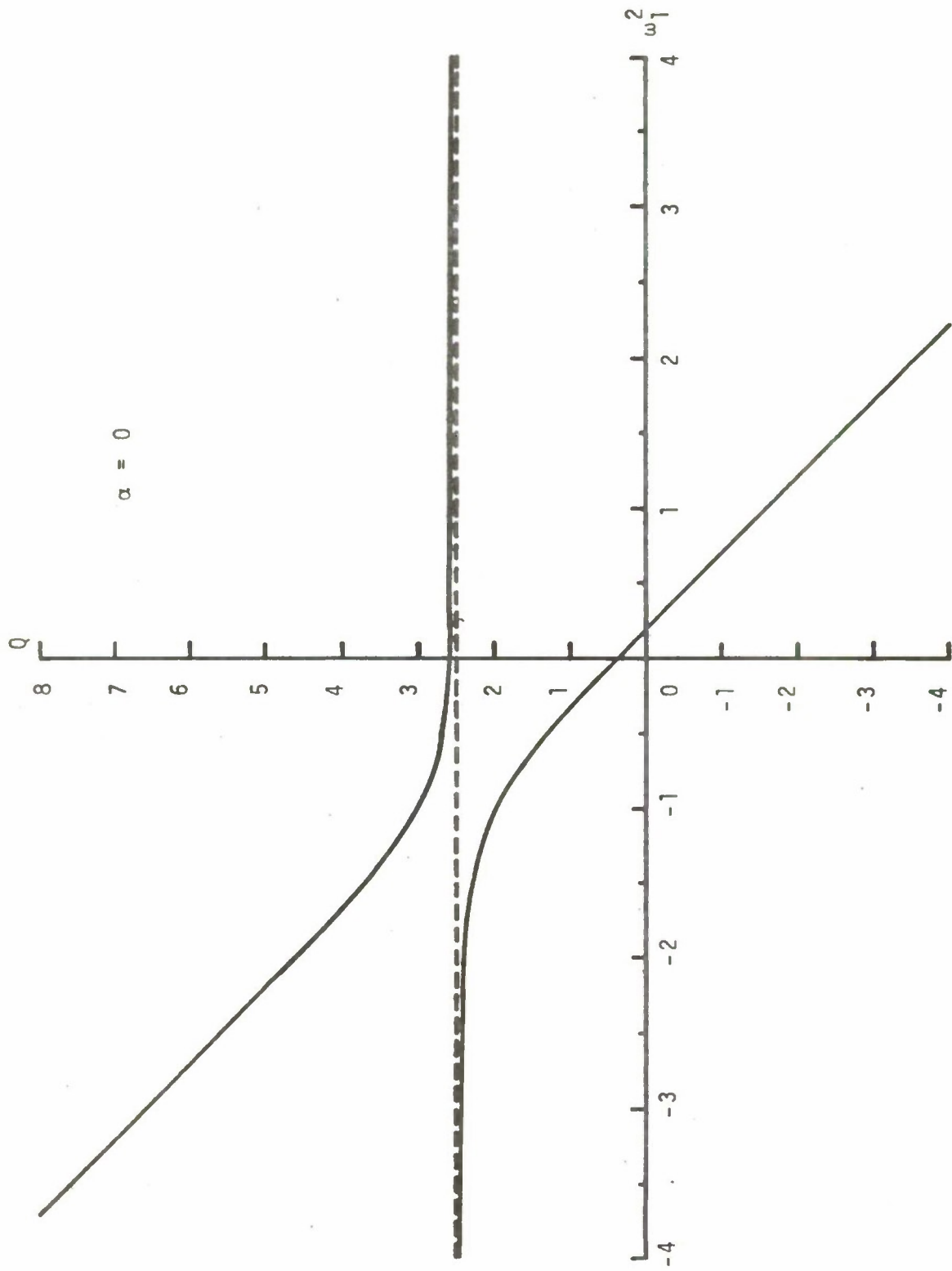


Figure 2a. Eigencurves for  $\alpha = 0$ .

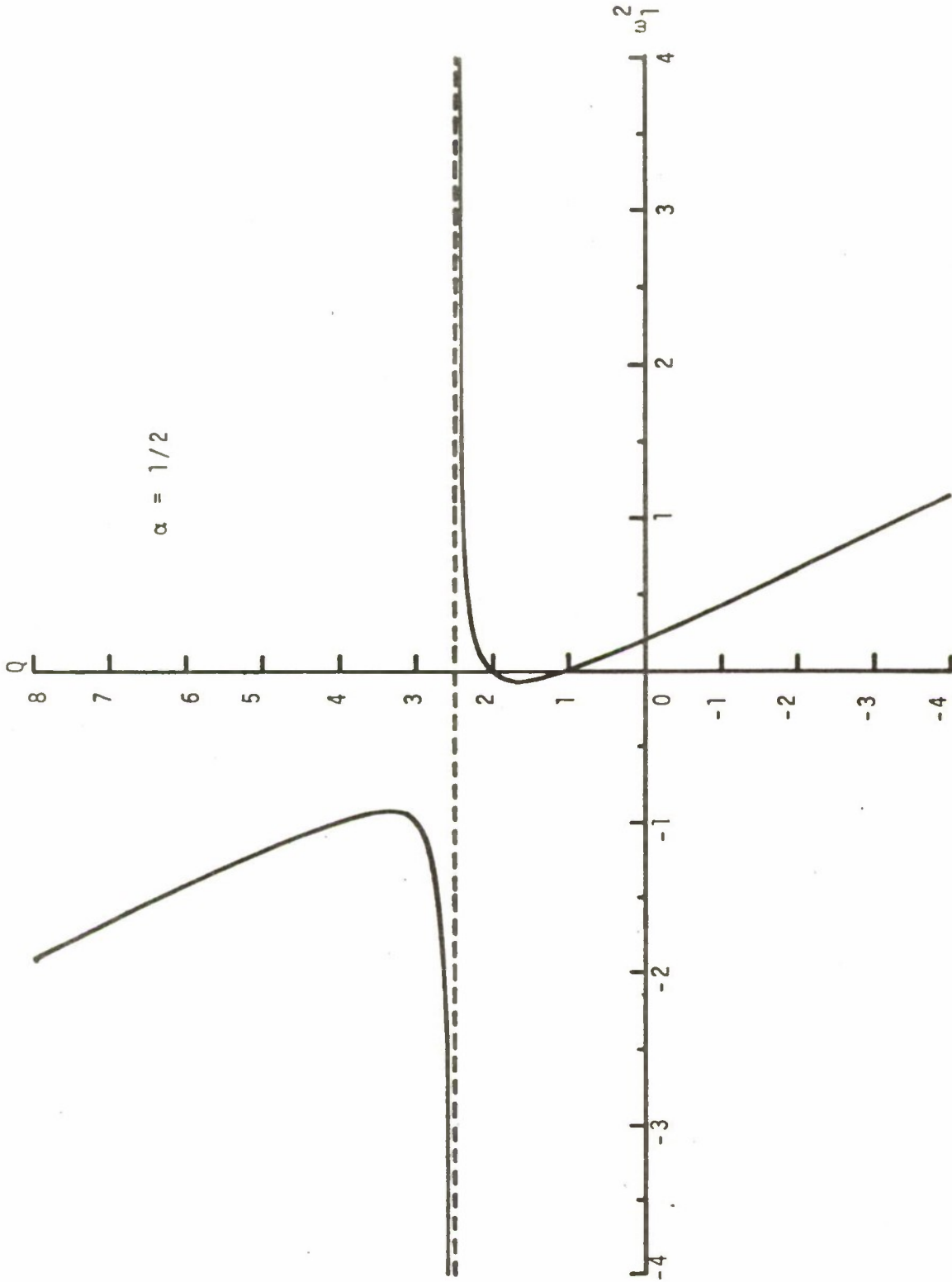


Figure 2b. Eigencurves for  $\alpha = 1/2$ .

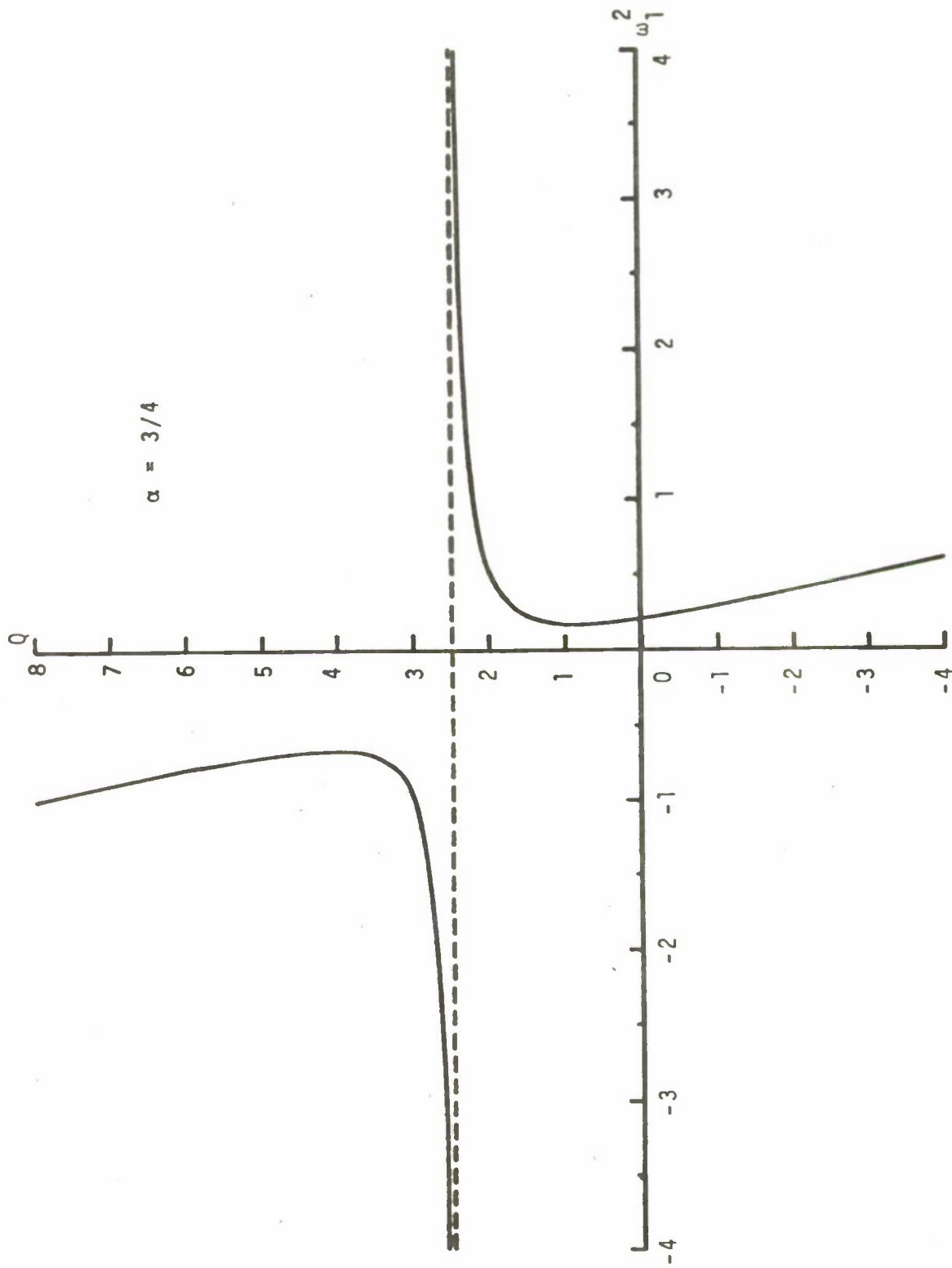


Figure 2c. Eigencurves for  $\alpha = 3/4$ .

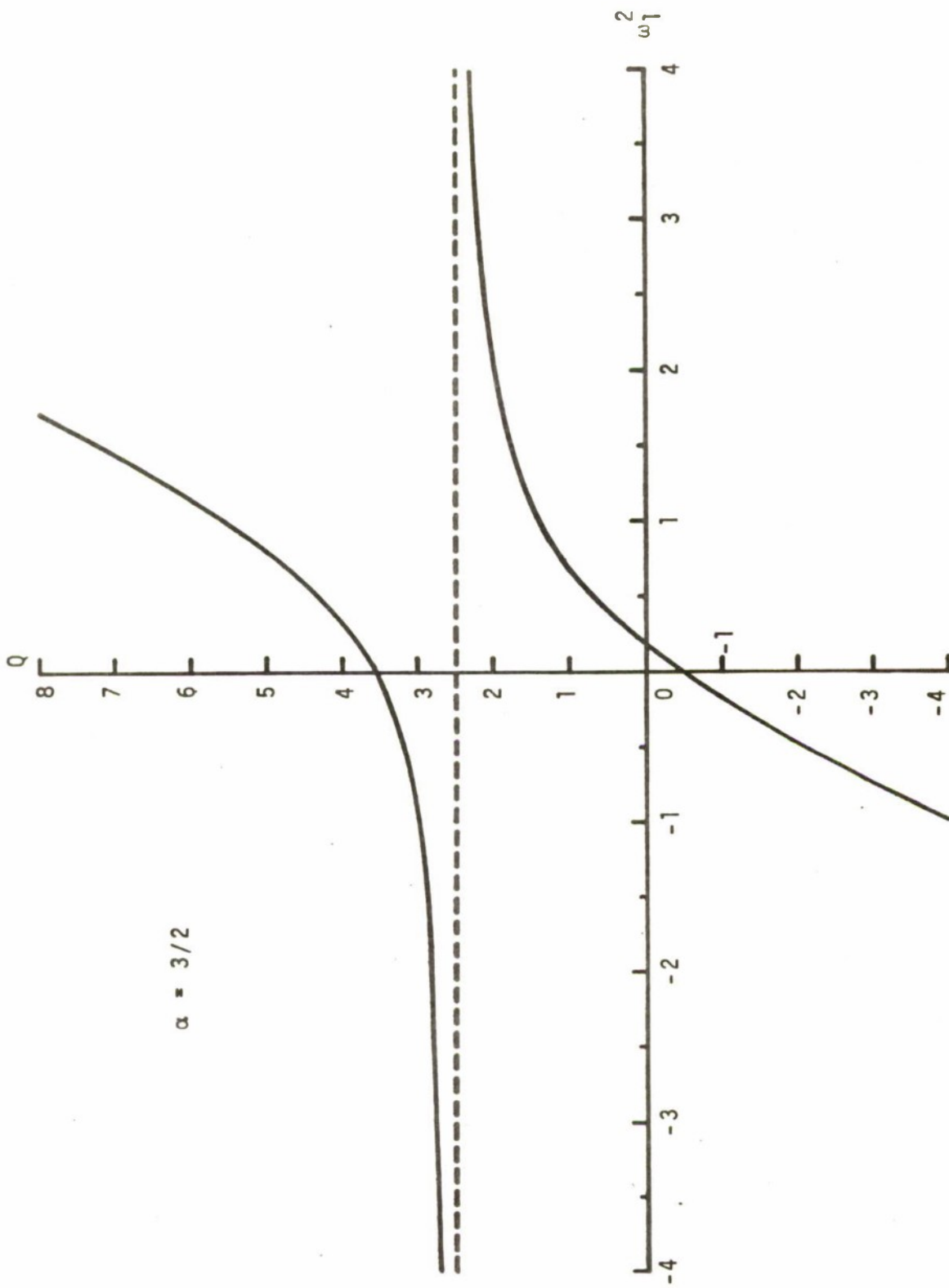


Figure 2d. Eigencurves for  $\alpha = 3/2$ .

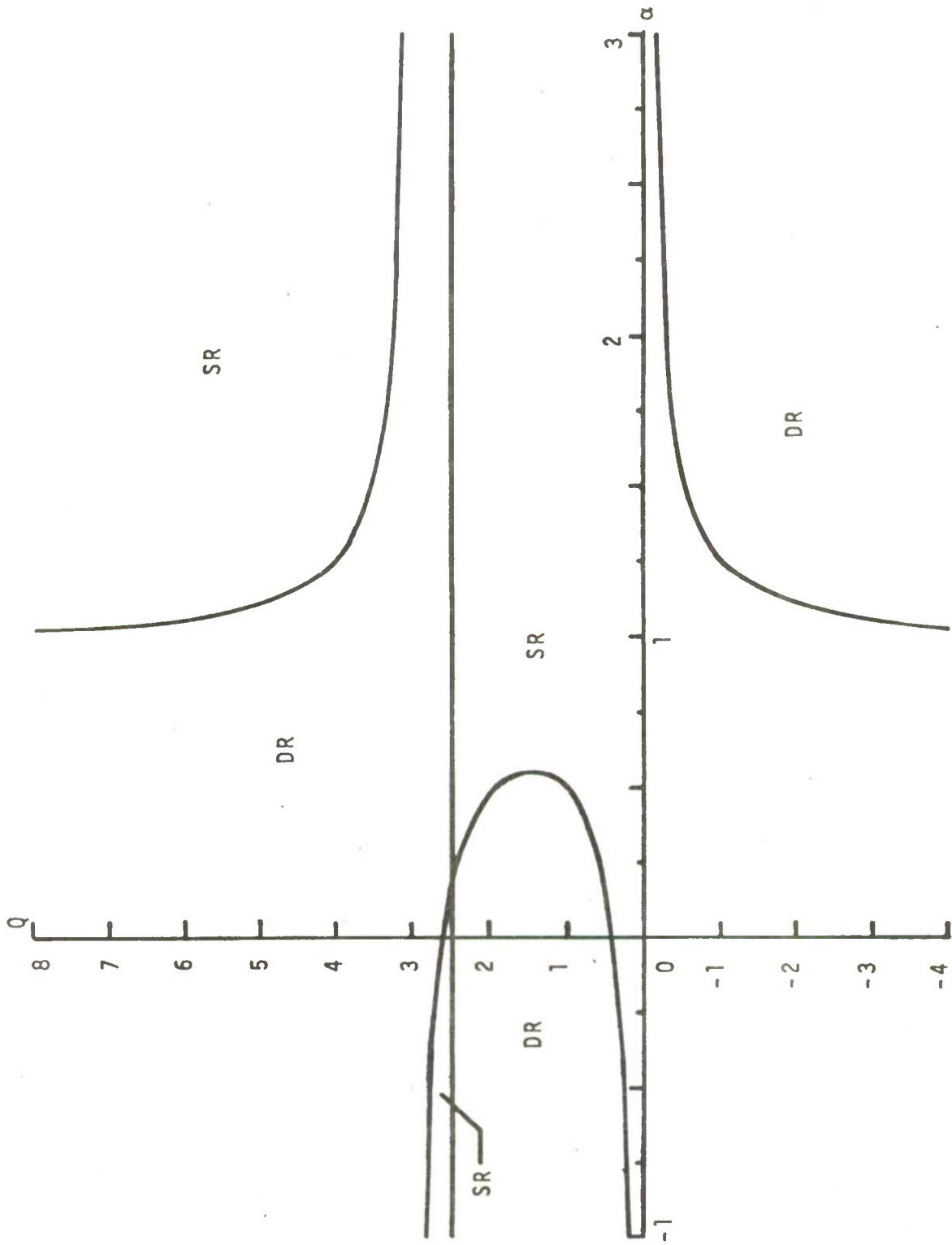


Figure 3. Stability map for a quasi-dynamic system ( $k_1=k_2=G=0$ ).

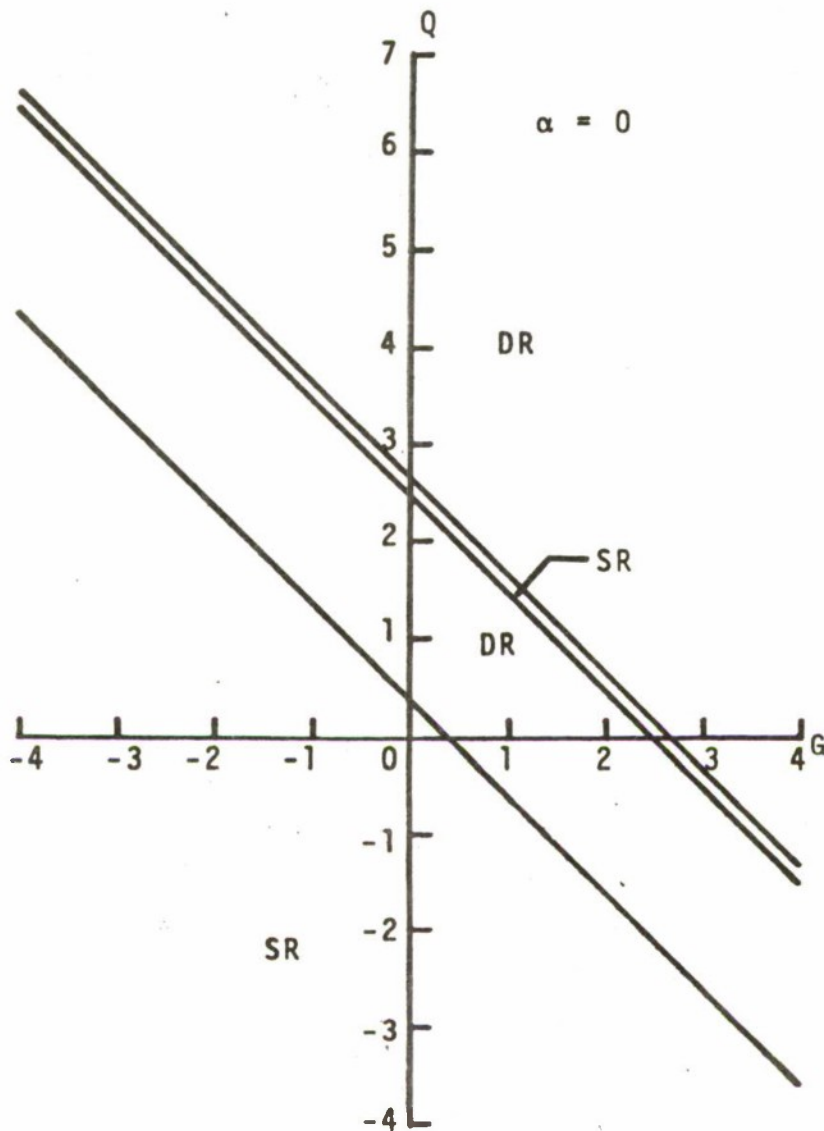


Figure 4a. The influence of weight on the stability of a quasi-dynamic system for  $\alpha = 0$  ( $k_1=k_2=0$ ).

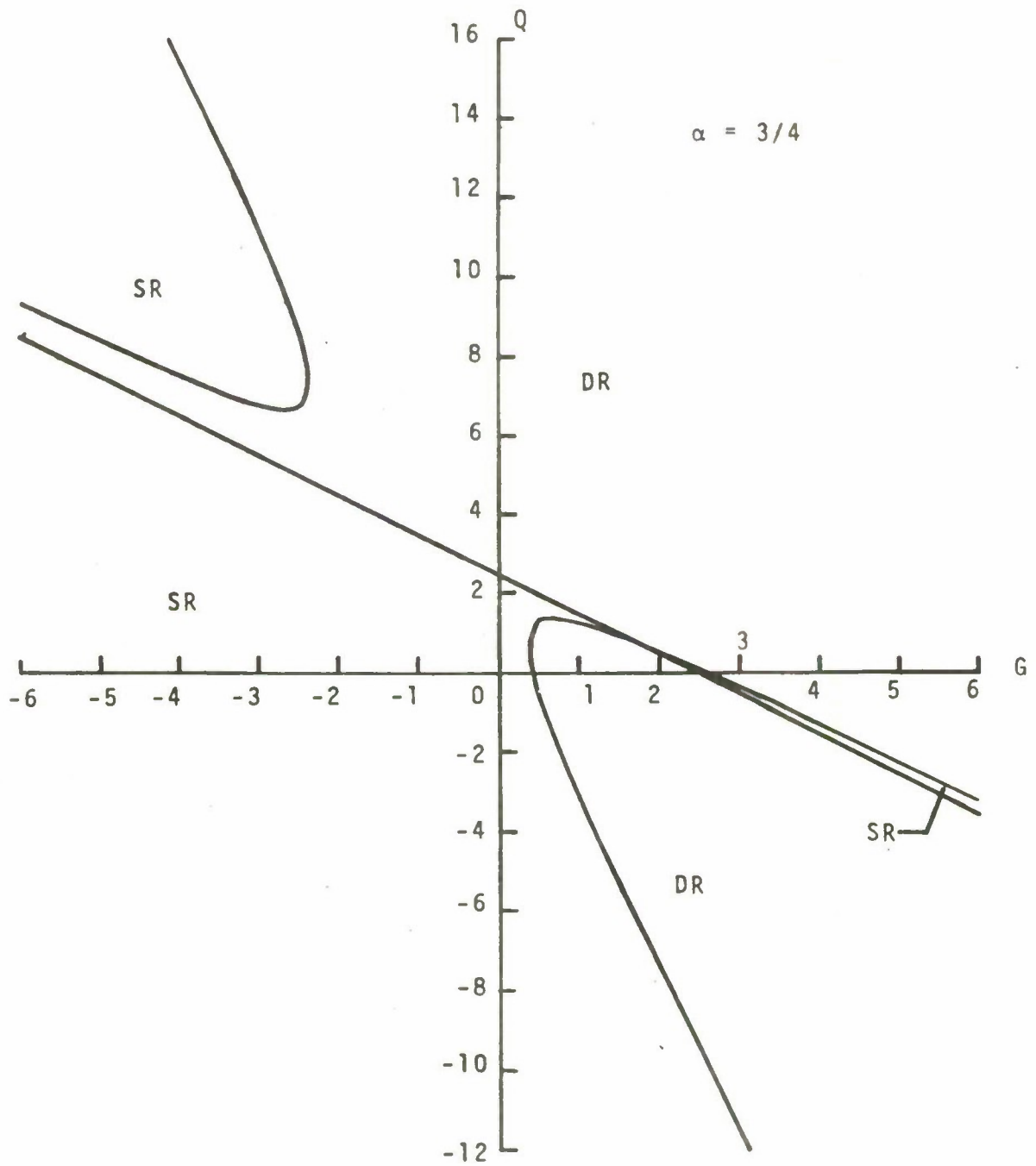


Figure 4b. The influence of weight on the stability of a quasi-dynamic system for  $\alpha = 3/4$  ( $k_1=k_2=0$ ).

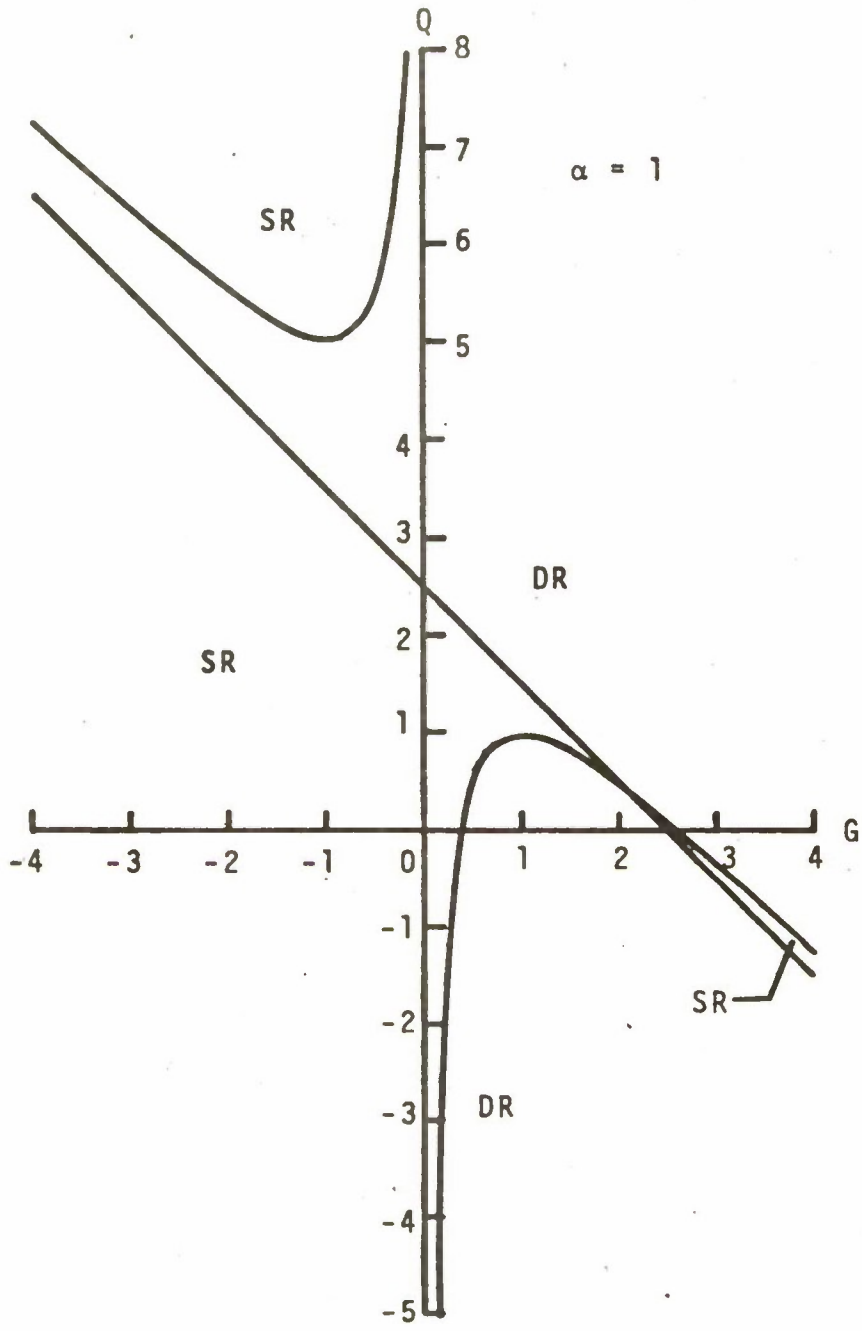


Figure 4c. The influence of weight on the stability of a quasi-dynamic system for  $\alpha = 1$  ( $k_1=k_2=0$ ).

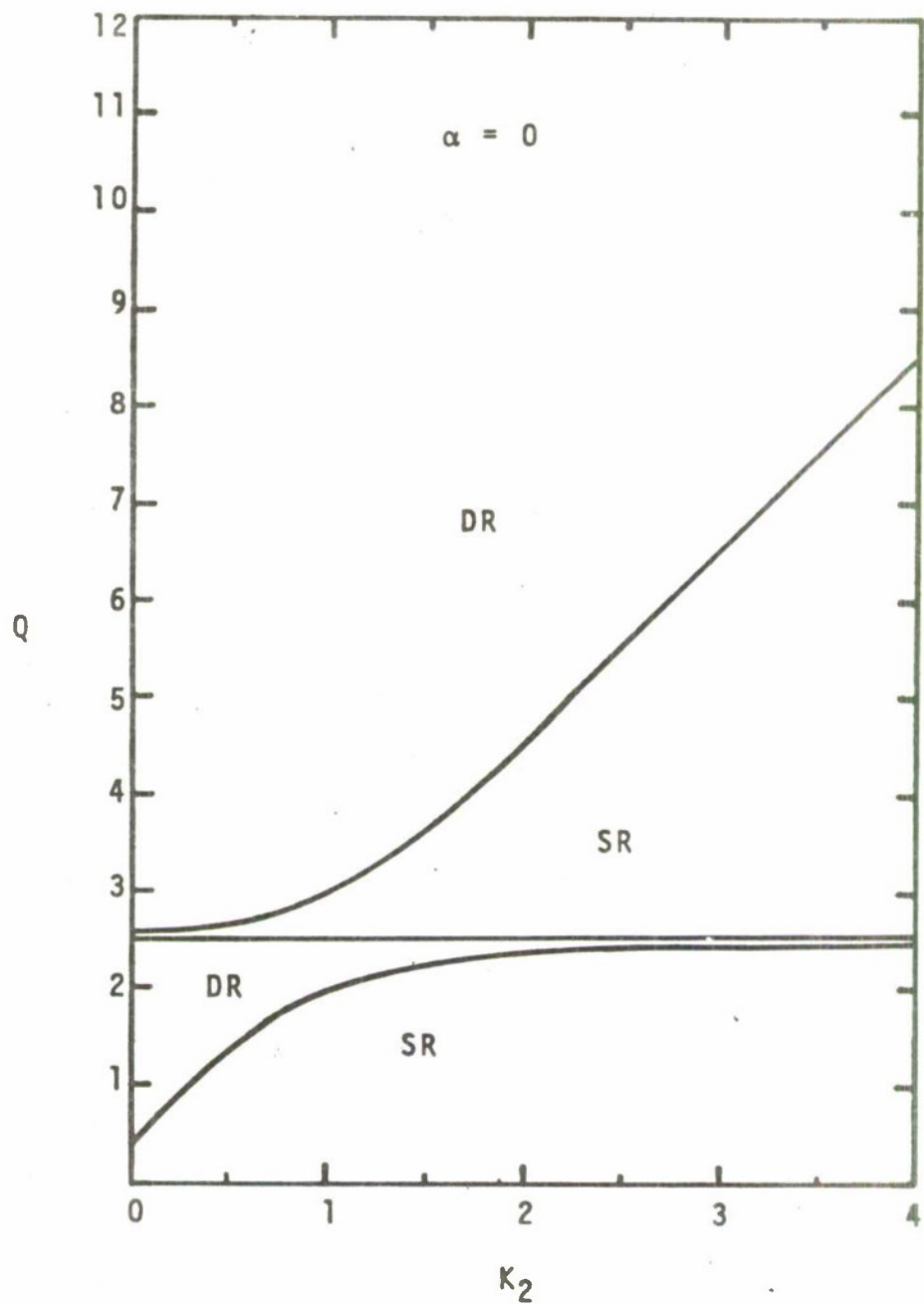


Figure 5a. Stability map for the system with an end constraint for  $\alpha = 0$  ( $G=k_1=0$ ).

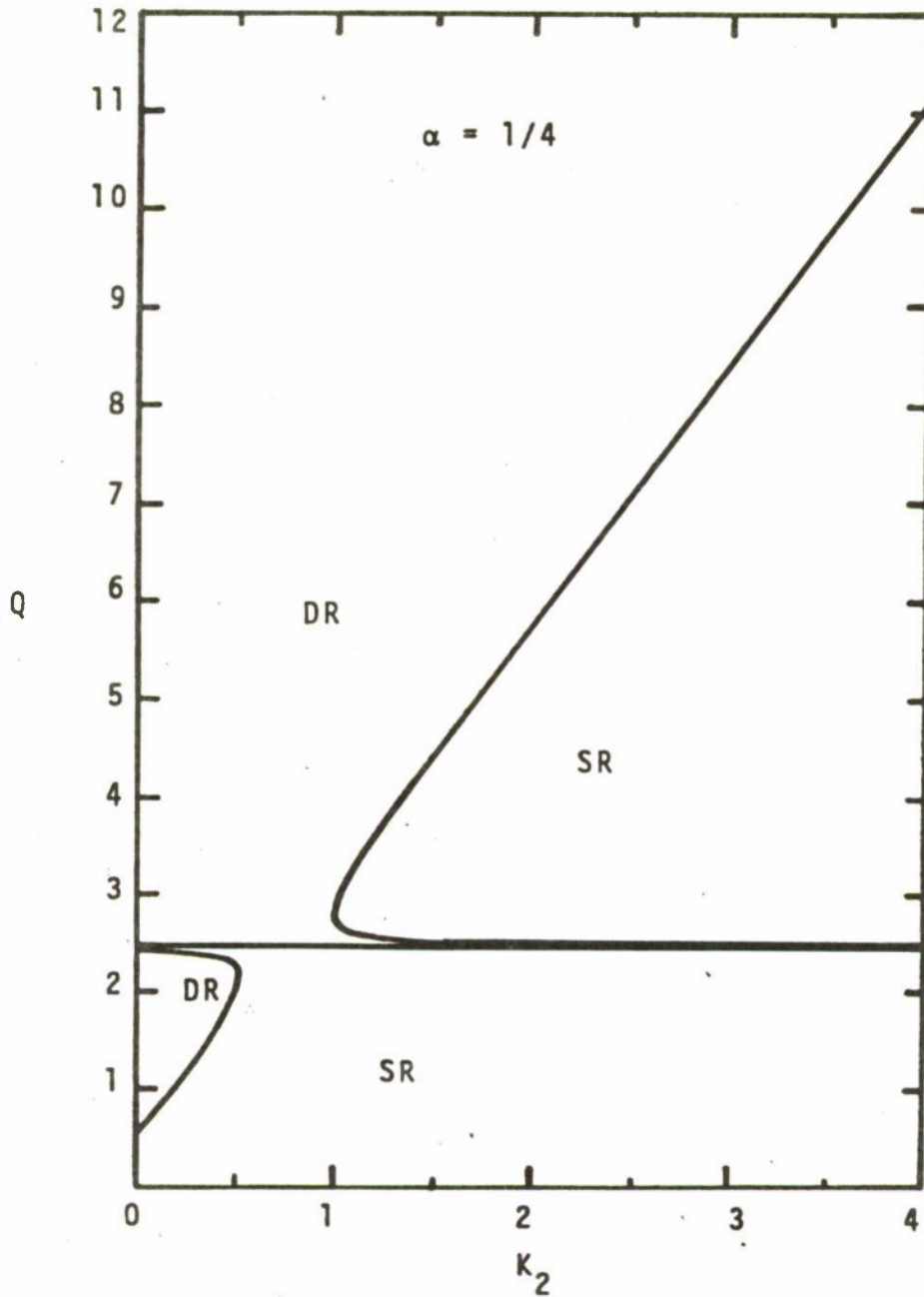


Figure 5b. Stability map for the system with an end constraint for  $\alpha = 1/4$  ( $G=k_1=0$ ).

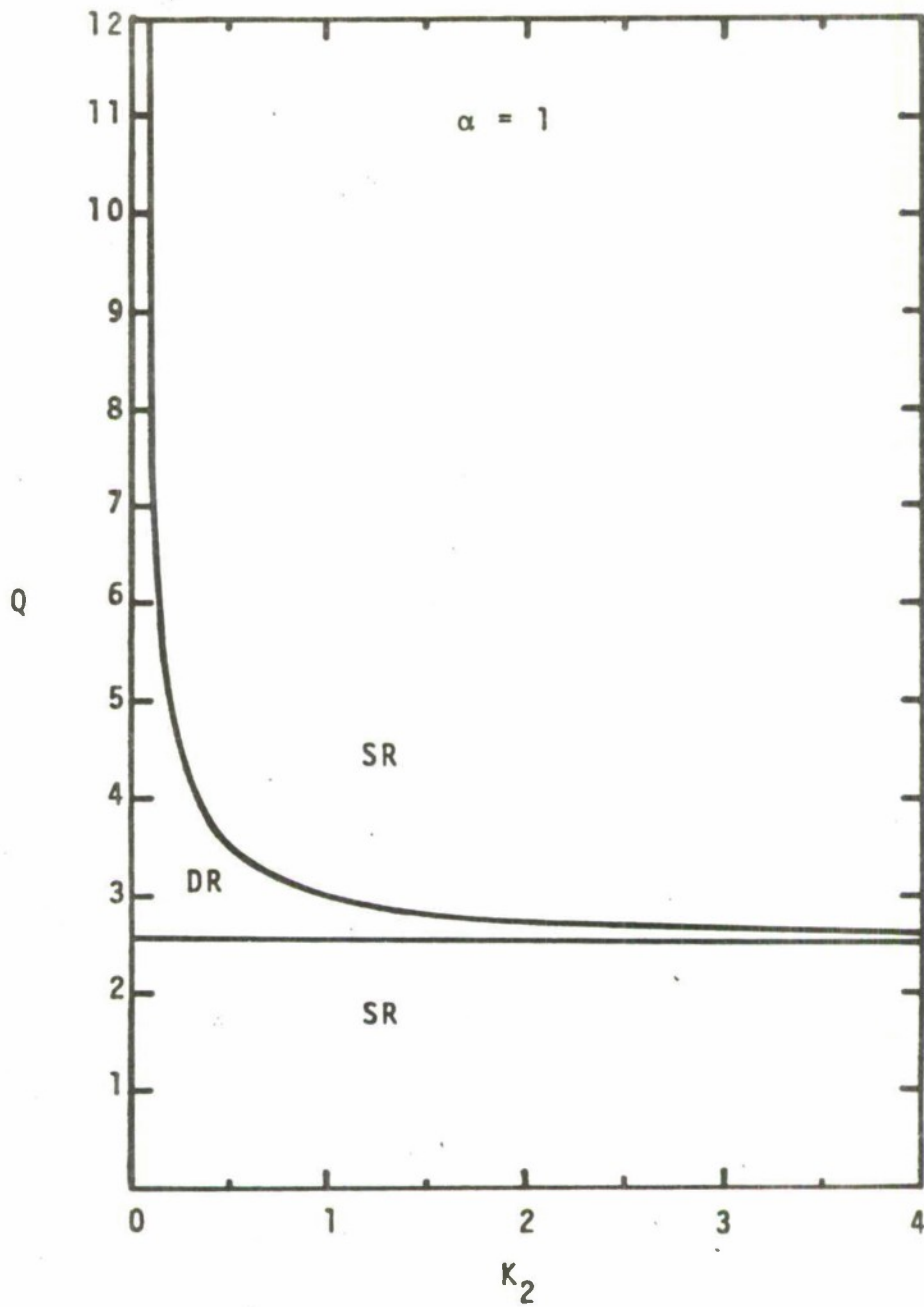


Figure 5c. Stability map for the system with an end constraint for  $\alpha = 1$  ( $G=k_1=0$ ).

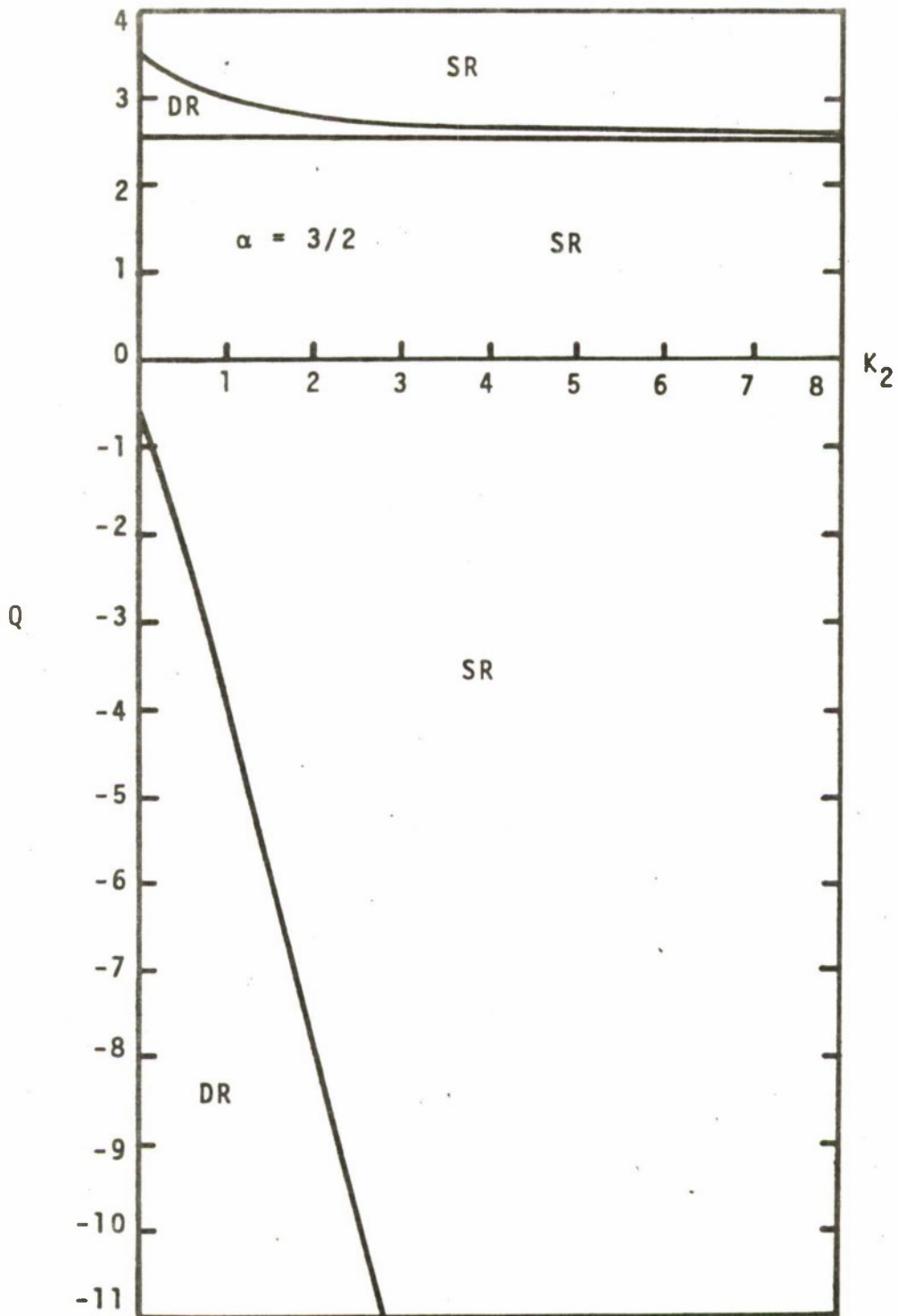


Figure 5d. Stability map for the system with an end constraint for  $\alpha = 3/2$  ( $G=k_1=0$ ).

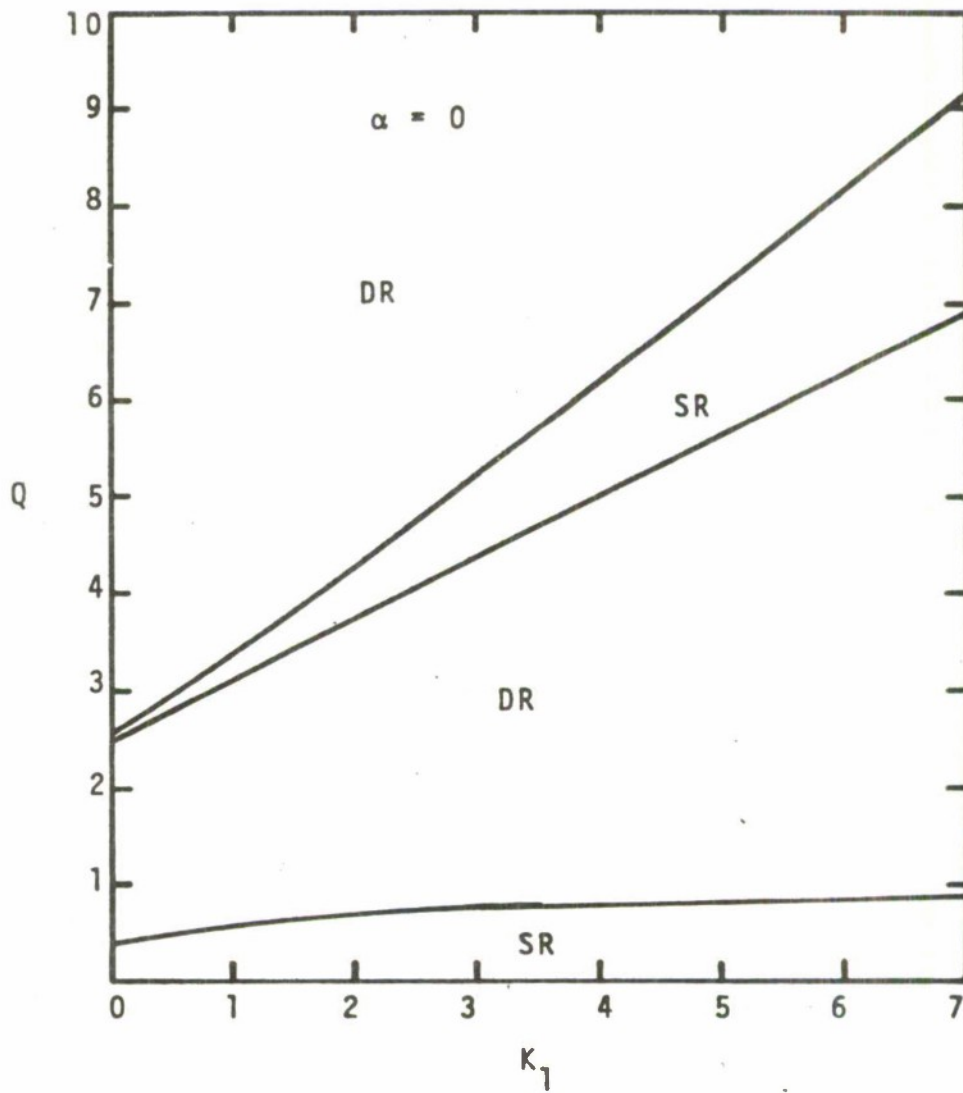


Figure 6a. Stability map for the system with a central constraint for  $\alpha = 0$  ( $G=k_2=0$ ).

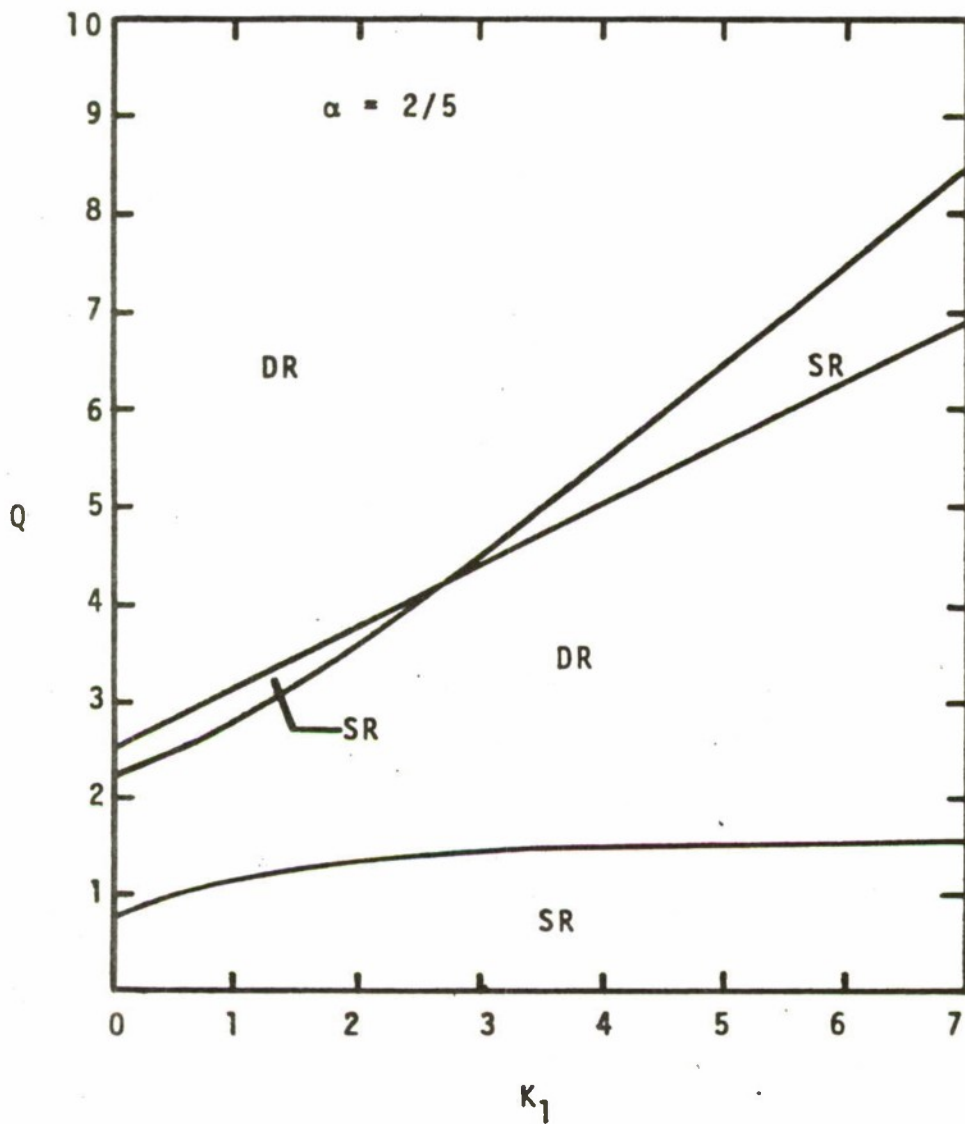


Figure 6b. Stability map for the system with a central constraint for  $\alpha = 2/5$  ( $G=k_2=0$ ).

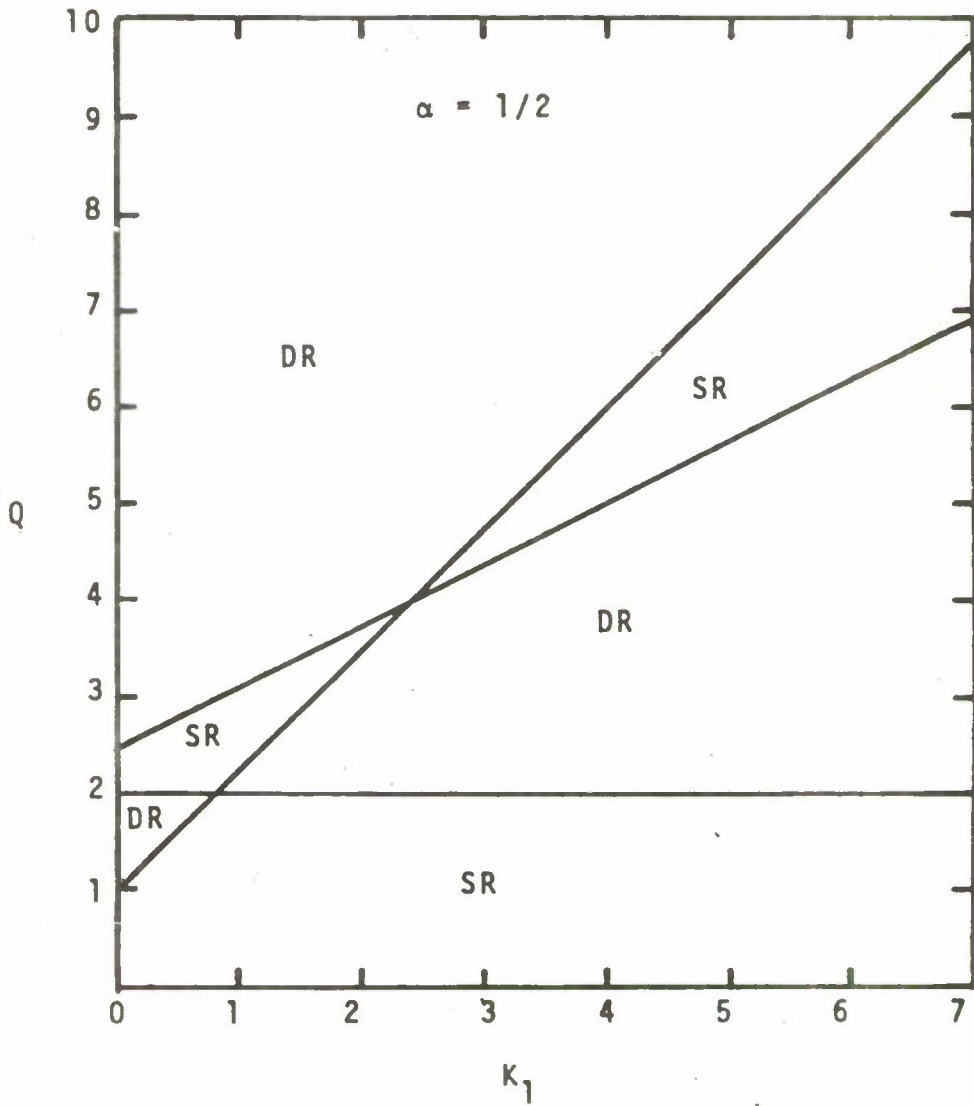


Figure 6c. Stability map for the system with a central constraint for  $\alpha = 1/2$  ( $G=k_2=0$ ).

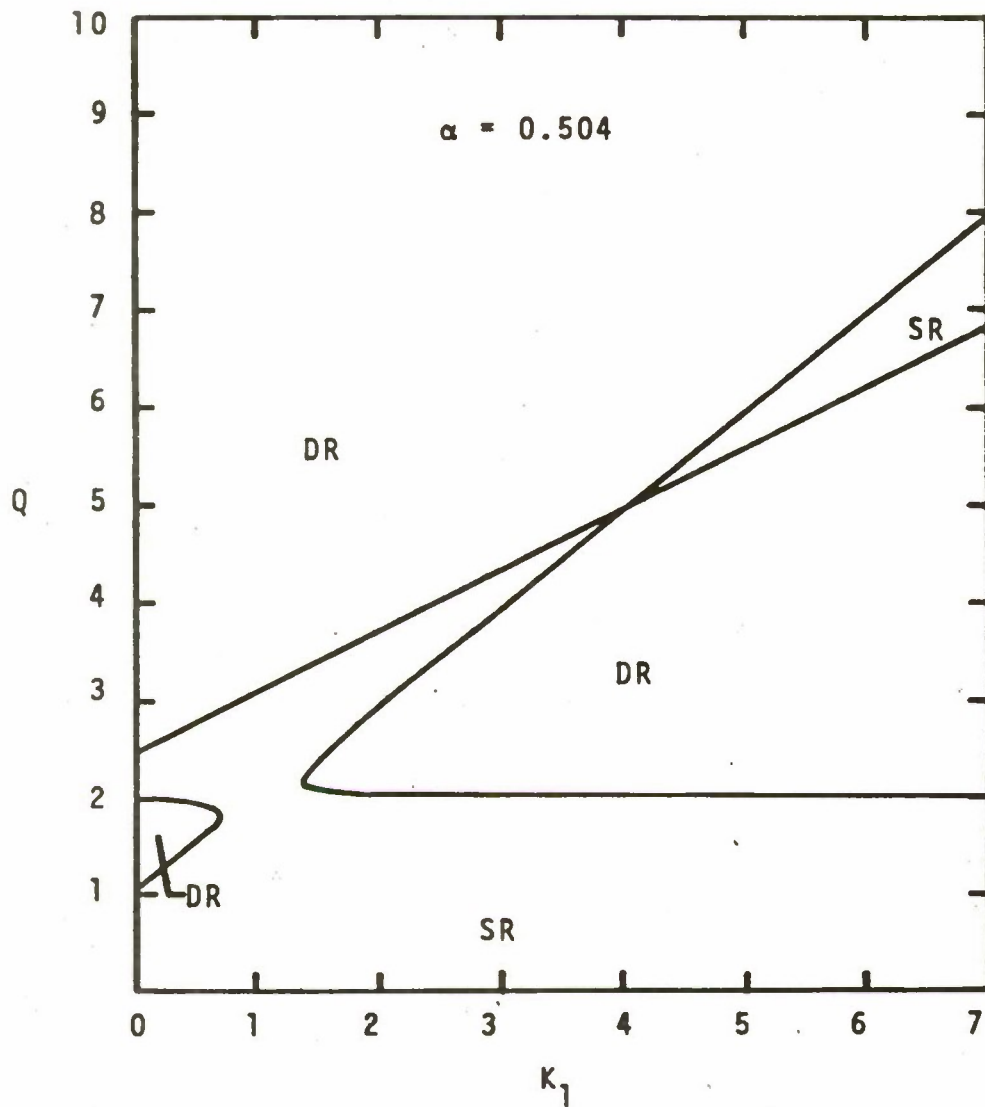


Figure 6d. Stability map for the system with a central constraint for  $\alpha = 0.504$  ( $G = k_2 = 0$ ).

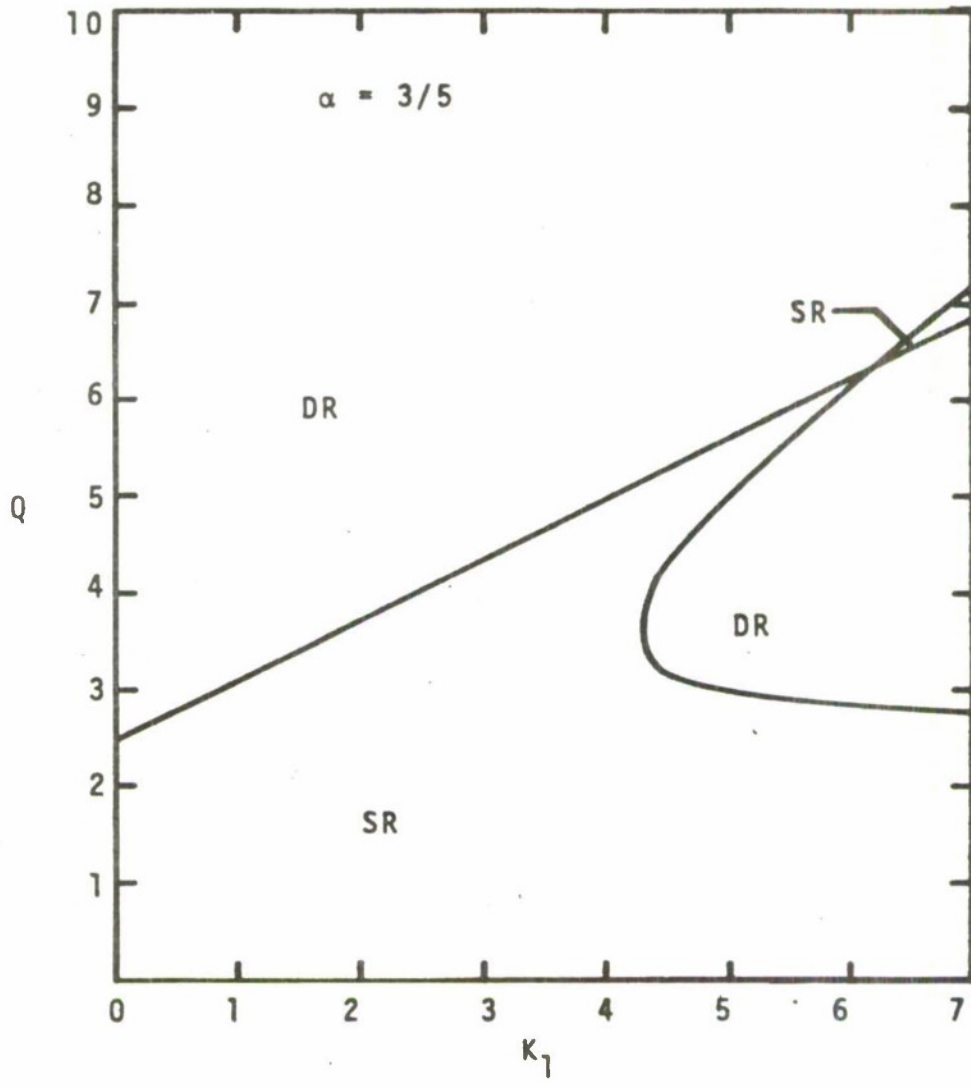


Figure 6e. Stability map for the system with a central constraint for  $\alpha = 3/5$  ( $G=k_2=0$ ).

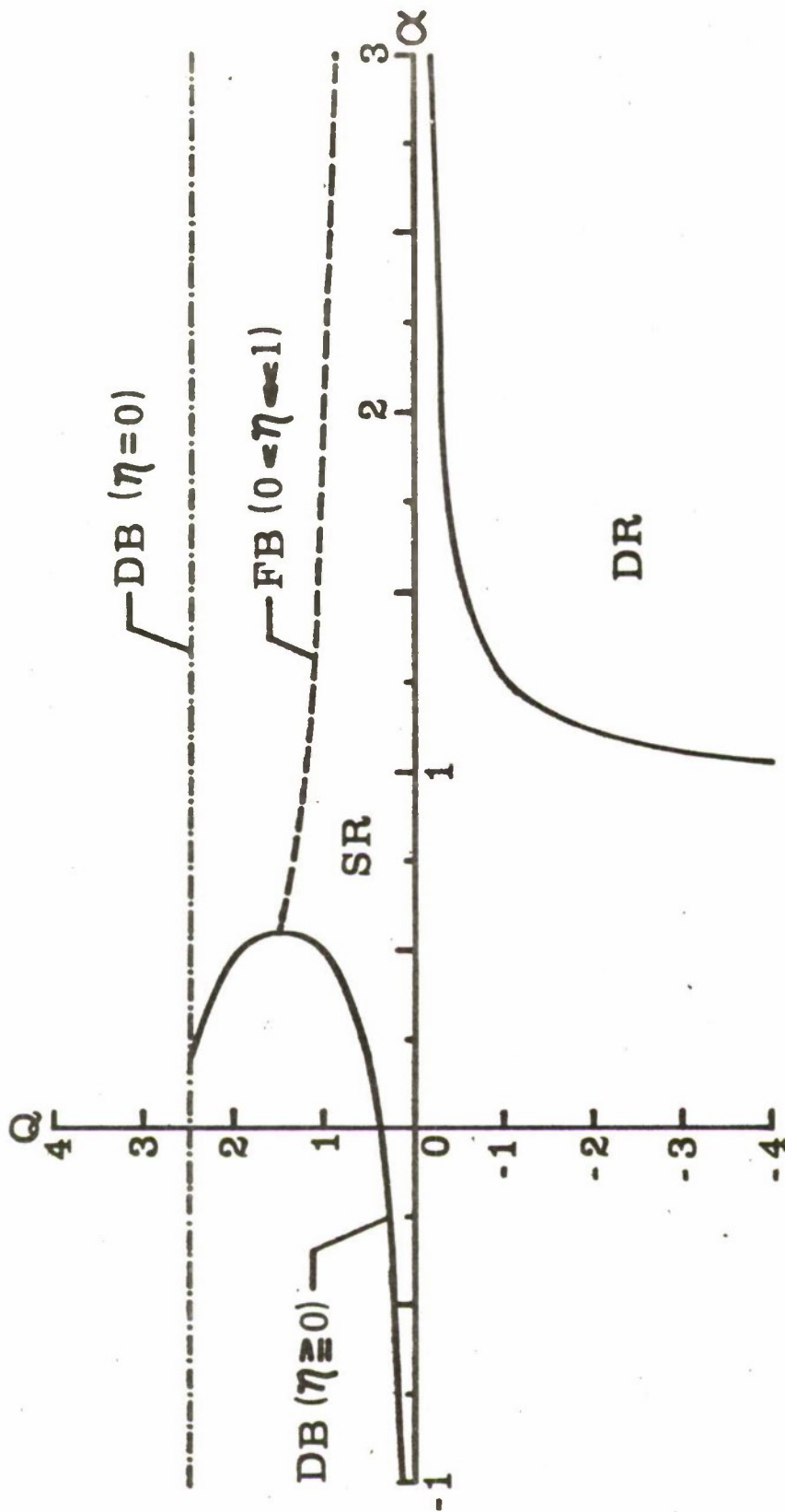


Figure 7. Stability map for a slightly damped system ( $k_1=k_2=G=0$ ).

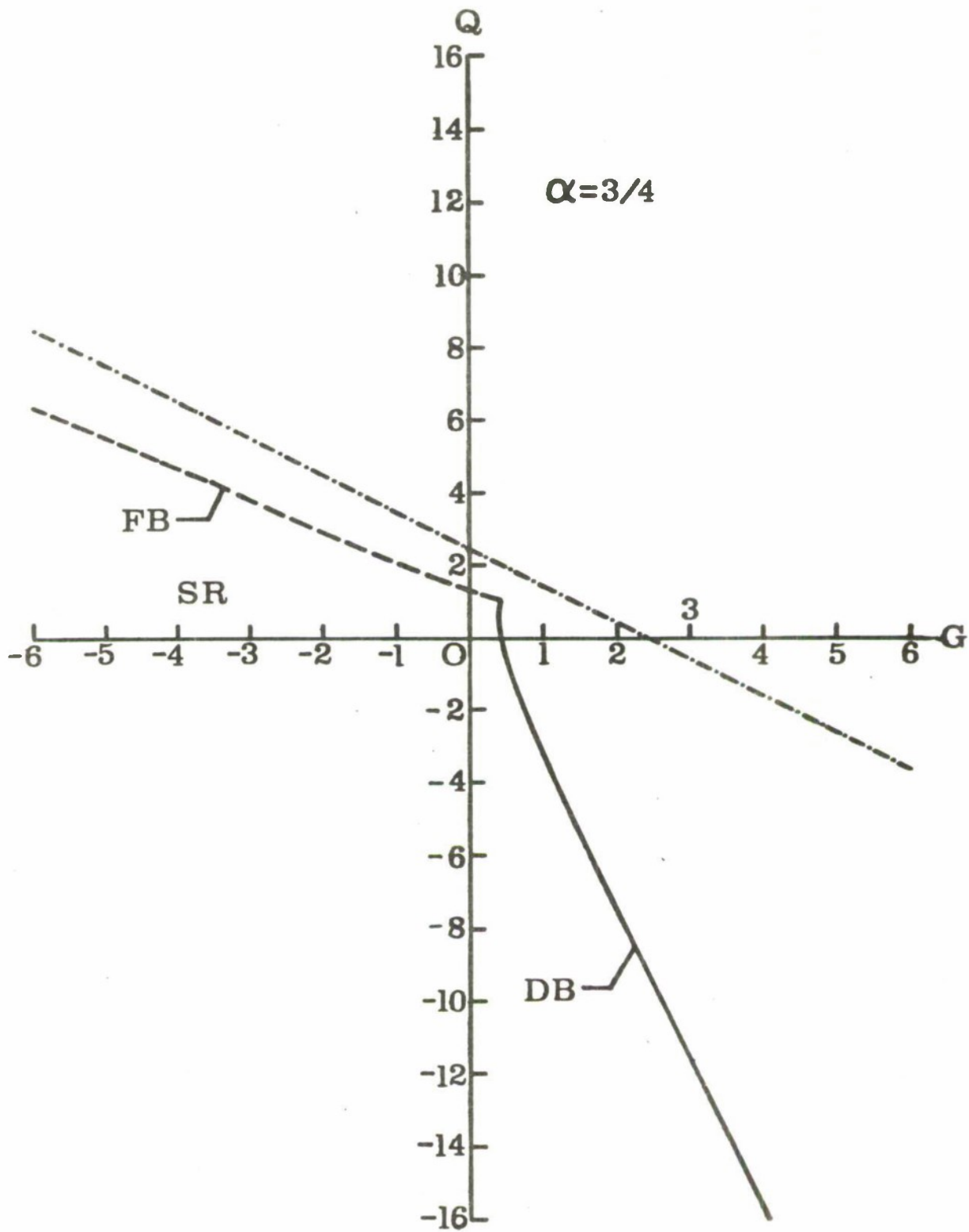


Figure 8a. The influence of weight on the stability of a slightly damped system for  $\alpha = 3/4$  ( $k_1 = k_2 = 0$ ).

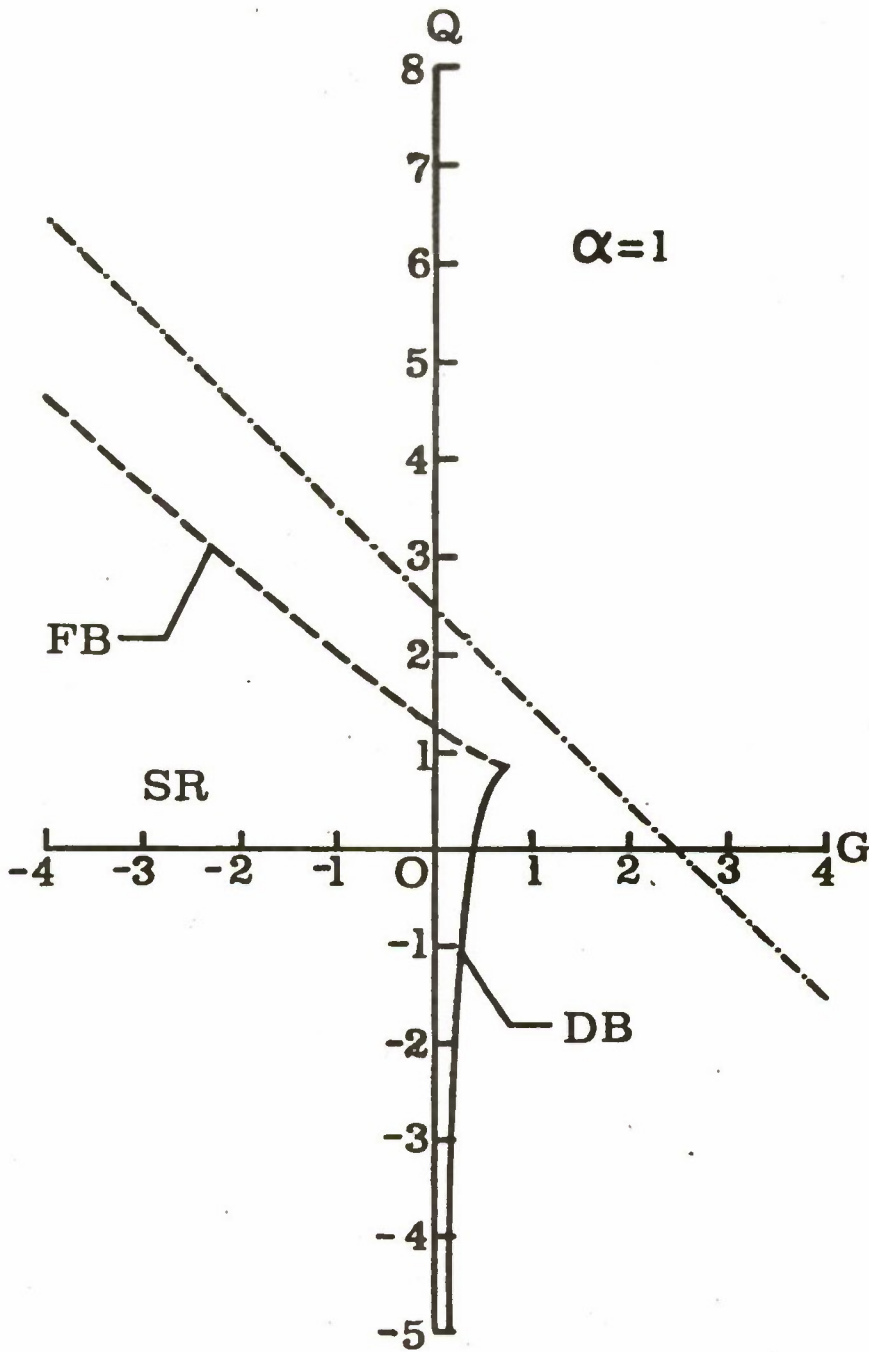


Figure 8b. The influence of weight on the stability of a slightly damped system for  $\alpha = 1$  ( $k_1=k_2=0$ ).

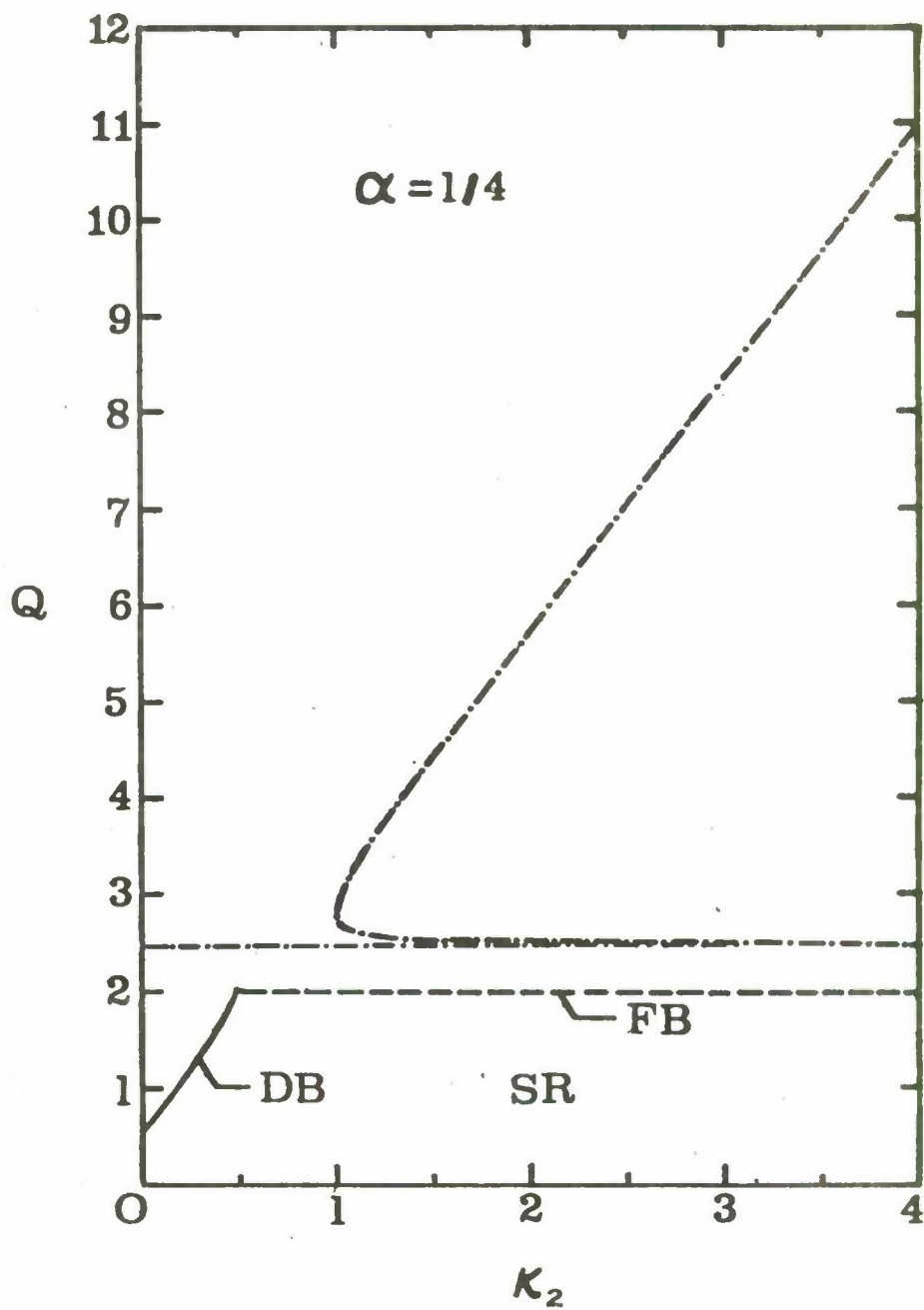


Figure 9a. Stability map for the slightly damped system with an end constraint for  $\alpha = 1/4$  ( $G=k_1=0$ ).

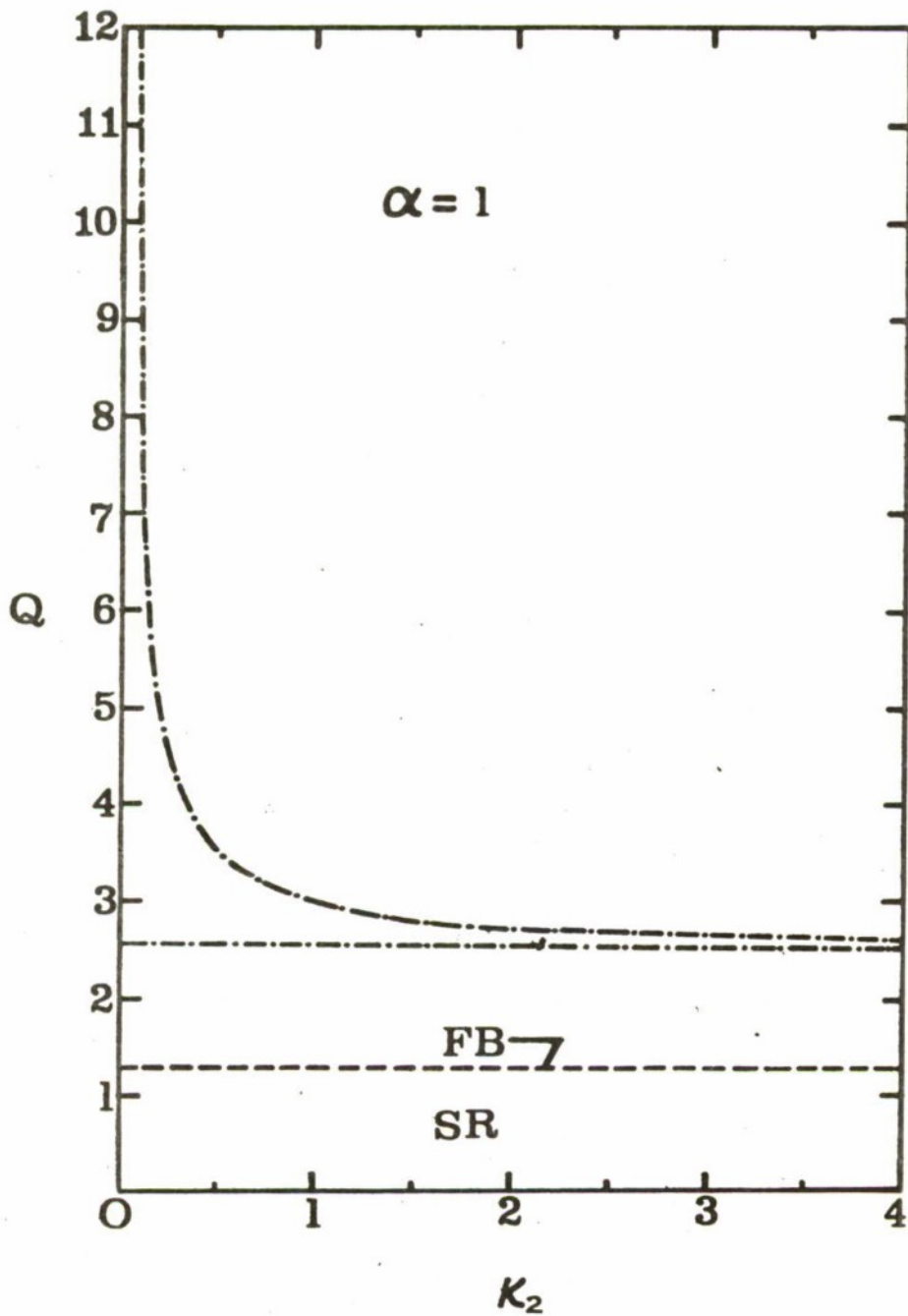


Figure 9b. Stability map for the slightly damped system with an end constraint for  $\alpha = 1$  ( $G=k_1=0$ ).

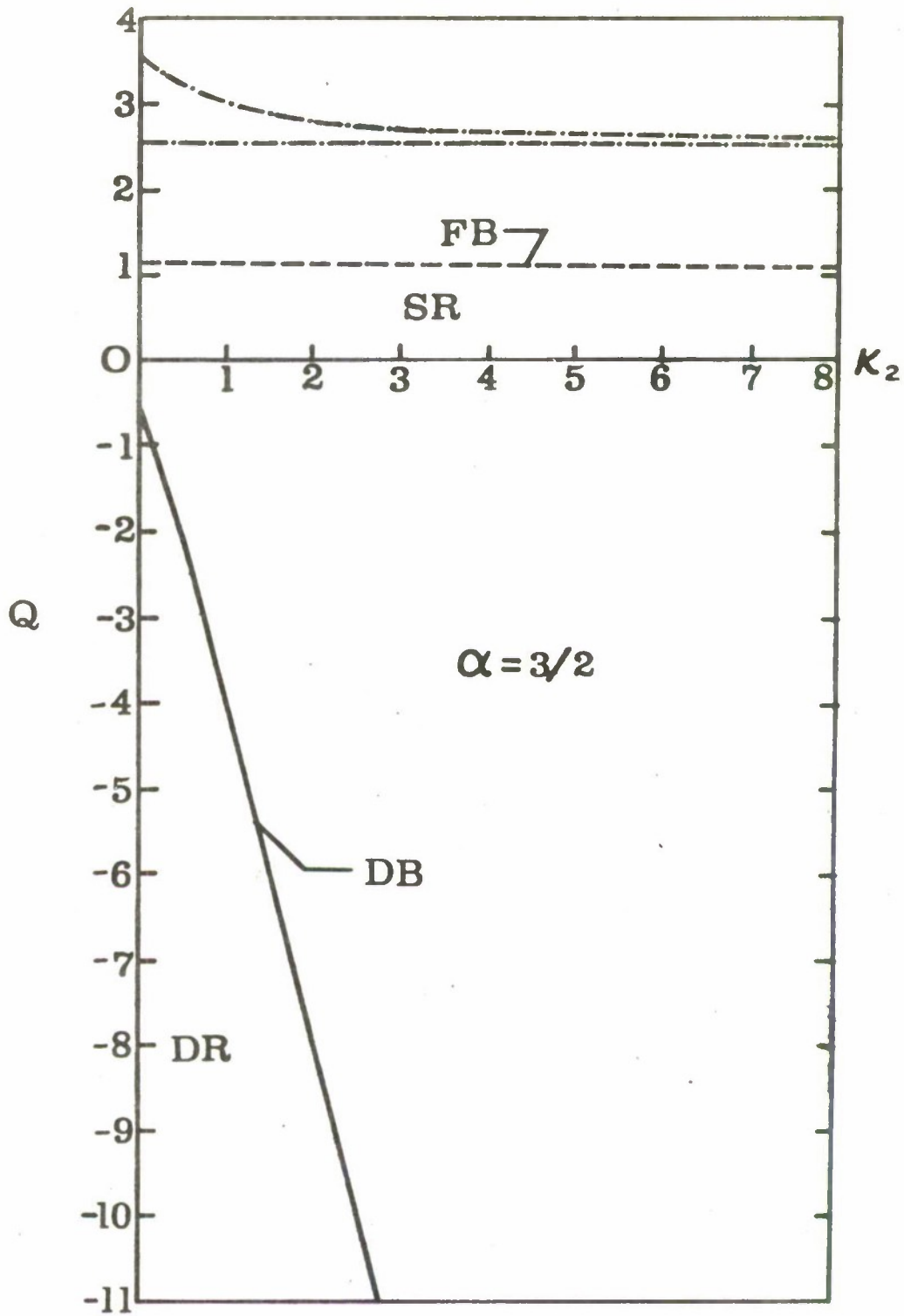


Figure 9c. Stability map for the slightly damped system with an end constraint for  $\alpha = 3/2$  ( $G=k_1=0$ ).

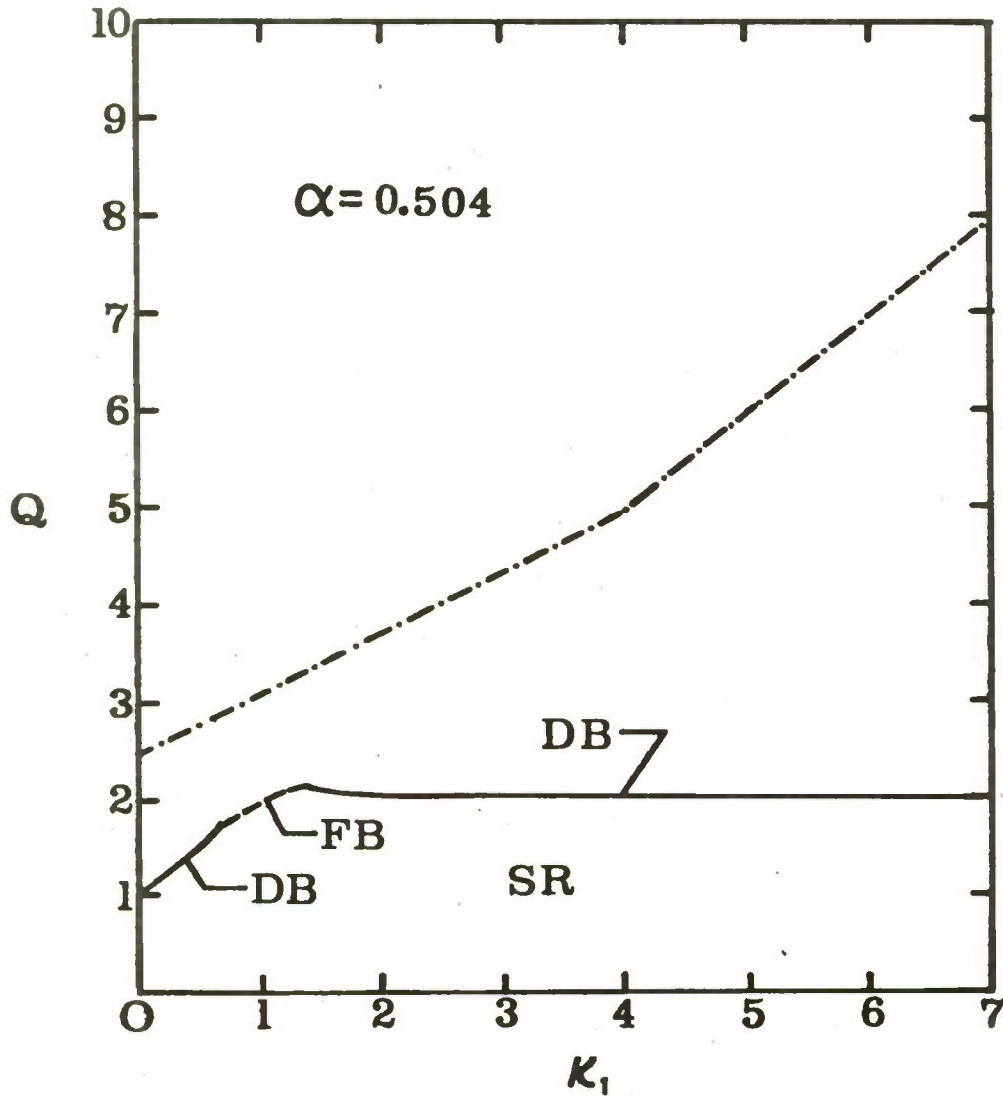


Figure 10a. Stability map for the slightly damped system with a central constraint for  $\alpha = 0.504$  ( $G=k_2=0$ ).

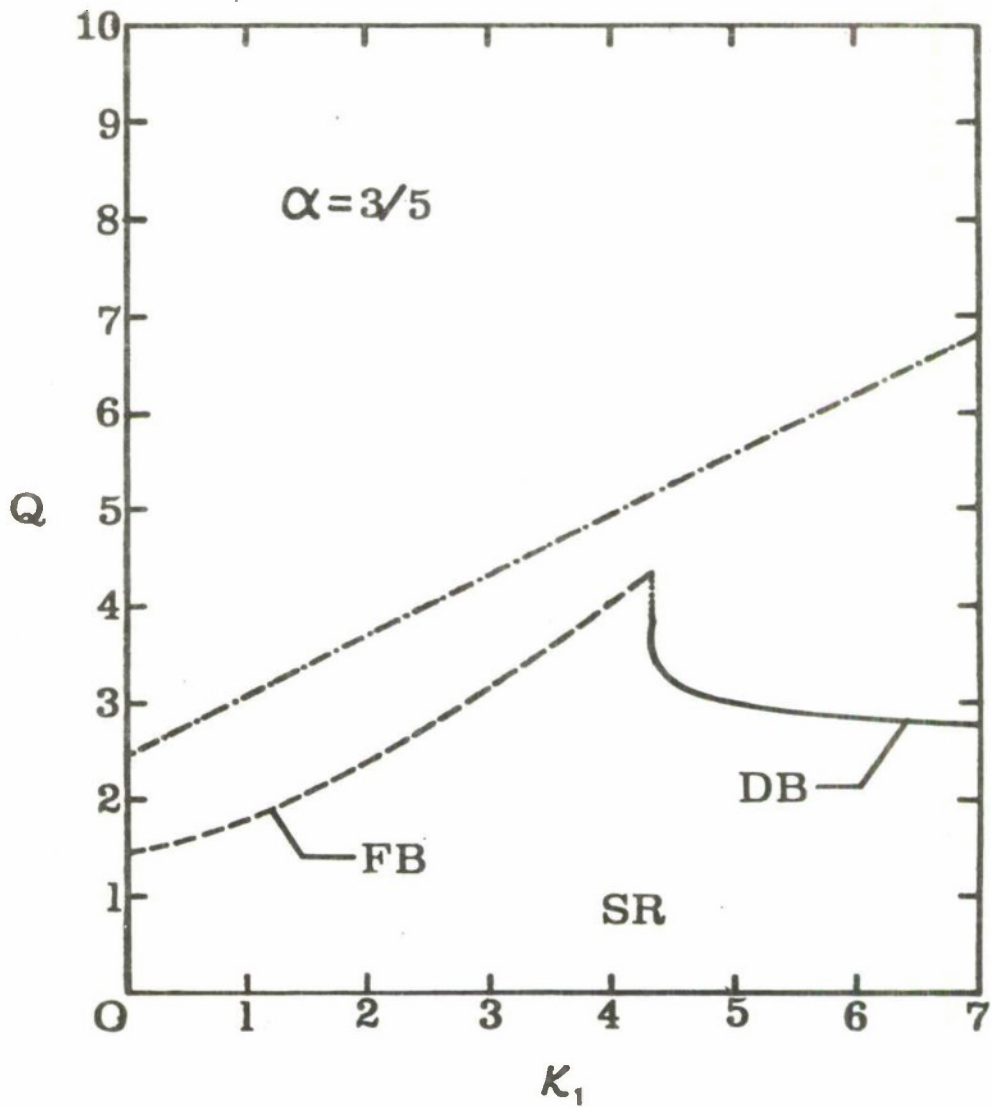


Figure 10b. Stability map for the slightly damped system with a central constraint for  $\alpha = .3/5$  ( $G=k_2=0$ ).